2007

Experimental and analytical modeling of the in vivo and in vitro biomechanical behavior of the human lumbar spine

Tov I. Vestgaarden
University of South Florida

Experimental and Analytical Modeling of the *In Vivo* and *In Vitro* Biomechanical Behavior of the Human Lumbar Spine

by

Tov I. Vestgaarden

A dissertation submitted in partial fulfillment
of the requirements for the degree of
Doctor of Philosophy
in Biomedical Engineering
Department of Chemical Engineering
College of Engineering
University of South Florida

Co-Major Professor: William E. Lee III, Ph.D.
Co-Major Professor: Antonio E. Castellvi, M.D.
Daniel Hess, Ph.D.
Ashok Kumar, Ph.D.
Shuh Jing Benjamin Ying, Ph.D.

Date of Approval:
November 2, 2007

Keywords: lumbar spine, biomechanics, intradiscal pressure, physiological loads, disc degeneration, spine fusion, posterior instrumentation, disc stresses, adjacent disc, facet fixation.

DEDICATION

I would like to dedicate this dissertation to my mom, dad, brother and sister; without their support I would not have had the courage to begin this adventure, or the strength to finish it. Thank You.

ACKNOWLEDGEMENTS

I would like to thank my parents, brother and sister for the continuous support during my years at University of South Florida. Without their love and support, this would not be possible. I would like to thank the people and institutions that supported me during my years as a graduate student at University of South Florida.

My heartfelt thanks go to Dr. William E. Lee III and Dr. Antonio E. Castellvi for their guidance and sponsorship for these research projects. I would also like to thank my examining committee Dr. Daniel Hess, Dr. Ashok Kumar and Dr. Shuh-Jing Ying for taking their valuable time to be involved in this project.

A special note of recognition goes to Dr. David Pienkowski, Dr. Hao Huang, Dr. Ke Li, Dr. Wes Johnson and Dr. Murray Maitland, for their valuable time, advice, guidance, and patience throughout this endeavor. I thank Deborah Clabeaux, for her help with numerous research and administrative tasks; without her nothing would be possible.

I would like to thank all my friends for all their support during my dad's fight against cancer. I would also like to thank MBNA for their 0% interest, so that continuing school has been possible after ended support. I would also like to thank my Godson, Jacob, and Goddaughter, Thea, for all the smiles.

Jeg vil også takke min familie for all hjelp og støtte gjennom min studie tid. Nå er det heldigvis ikke alt for lenge igjen, og da er det min tid til å hjelpe dere på alle mulige måter.

TABLE OF CONTENTS

LIST OF TABLES

LIST OF FIGURES

EXPERIMENTAL AND ANALYTICAL MODELING OF THE *IN VIVO* and *IN VITRO* BIOMECHANICAL BEHAVIOR OF THE HUMAN LUMBAR SPINE

Tov I. Vestgaarden

ABSTRACT

This dissertation has two major parts; Analytical and Experimental. The analytical section contains a study using Finite Element Analysis of dynamic instrumentation to demonstrate stress reduction in adjacent level discs. The experimental section contains biomechanical testing of facet fusion allograft technique and finally a comparison between *In Vivo* and *In Vitro* intradiscal pressures to determine forces acting on Lumbar spine segment L4-L5. A comprehensive study of available data, technology and literature was done.

Conventional fusion instrumentation is believed to accelerate the degeneration of adjacent discs due to the increased stresses caused by motion discontinuity. A three dimensional finite element model of the lumbar spine was obtained which simulated flexion and extension. Reduced stiffness and

increased axial motion of dynamic posterior lumbar fusion instrumentation designs results in a ~10% cumulative stress reduction for each flexion cycle. The cumulative effect of this reduced amplitude and distribution of peak stresses in the adjacent disc may partially alleviate the problem of adjacent level disc degeneration.

Traditionally a pedicle screw system has been used for fixation of the lumbar spine and this involves major surgery and recovery time. Facet fixation is a technique that has been used for stabilization of the lumbar spine. The cadaver segments were tested in axial rotation, combined flexion/extension and lateral bending. Implantation of the allograft dowel resulted in a significant increase in stiffness compared to control. Facet fusion allograft provides an effective minimally invasive method of treating debilitating pain caused by deteriorated facet joints by permanently fusing them.

An *In Vitro* biomechanical study was conducted to determine the intradiscal pressure during spinal loading. The intradiscal pressures in flexion/extension, lateral bending and axial rotation was compared to *In Vivo* published data. There is no data that explains the actual forces acting on the spine during flexion, extension, lateral bending or axial rotation. The functional spinal units were tested in combined axial compression and flexion/extension, combined axial compression and lateral bending and combined axial compression and axial rotation using a nondestructive testing method. Overall, this study found a good correlation between *In Vivo* and *In Vitro* data. This can

essentially be used to make physiological relation from experimental and analytical evaluations of the lumbar spine. It is important to know how much load needs to be controlled by an implant.

CHAPTER 1 – INTRODUCTION

1.1 – Background

First, I want to introduce some commonly used terms in medicine to describe directions, planes and motions. A person that is orientated in the “anatomical” position is facing forward, with arms and legs on a slight angle. The “palms of hands” are facing forward.

Directional terms commonly used are Anterior, Posterior, Superior, Inferior, Medial and Lateral. Anterior, also referred to as Ventral, means toward the front. Posterior (Dorsal) is towards the back, and as an example we can look at the vertebra. When you look at the vertebra, you have the vertebral body and the posterior elements. These posterior elements are towards the back. Superior (cranial) is towards the top and inferior (caudal) is towards the bottom. Medial describes the midline of the body and Lateral means away from the midline of the body.

In general there are three planes; frontal, midsagittal and transverse plane. The frontal plane is the plane that goes from inferior-superior and right-left. As an example, right side bending will occur within the frontal plane. The

other planes are midsagittal (anterior-posterior and inferior-superior) and transverse (anterior-posterior and right to left) planes.

1.1.1 – Spine Anatomy

1.1.1.1 – Normal Curves

The spine consists of four curvatures, and they alter between convex and concave. The cervical region (neck) has a concave curvature and the same does the lumbar region (lower back). The thoracic region (mid region) and Sacral region are both convex curved.

Figure 1-1: The Complete Human Spine

1.1.1.2 – Curvature Abnormalities

There are some curvature abnormalities that might be present at birth, while others might be the caused from a disease, uneven muscle force or bad posture. The most frequently seen curvature abnormalities are scoliosis, kyphosis and lordosis.

Scoliosis is a spine curvature that is abnormal in the lateral curvature and the spine should normally be straight in this position. While the spine will always have a slight scoliosis (lateral curvature in the frontal plane), it will not cause problems with most people. Scoliosis is more common for females and is most common to occur in late childhood.

Kyphosis is a change in the thoracic curvature towards the back (posterior). The spine is rounded, and the vertebral bodies are usually compressed into a wedge shape. This is most commonly caused by compression fractures due to osteoporosis.

Lordosis is an exaggerated lumbar curvature and is often referred to swayback.

1.1.1.3 – Divisions

Three of these four regions are build up from vertebral and intervertebral disc. The vertebrae consist of a vertebral body, lamina, pedicle, spinous process, transverse process, superior facet and inferior facet. The disc that

connects the vertebral bodies is made from an incompressible center named nucleus pulposus and the nucleus pulposus is surrounded by the annulus fibrosus. The annulus fibrosus is build up by annulus grounds and layers of annulus fibers. These fibers have an alternating mesh that is aligned at an approximate 30 degrees.

1.1.1.4 – Typical Vertebra

Different regions have different characteristics to the vertebrae, but they have all some common features. A typical vertebra consists of the vertebral body, vertebral arch and seven processes.

The body is the solid construction of the vertebrae and is exposed to high compression loads. The majority of the loads are distributed through the vertebral body and the intervertebral disc act as the “shock absorber”. While the superior and inferior parts of the vertebral body are roughened for attachment of the intervertebral disc. The intervertebral disc is a thick, disc shaped construct. The anterior and posterior surfaces have ligaments running from superior to inferior on the spine. The anterior and lateral surfaces have nutrient foramina for blood vessels.

1.1.1.5 – Lumbar Vertebrae

The Lumbar vertebrae are the larges vertebrae in the spine. These are in the lower spine and carry the highest loads. A lumbar vertebra consists of the body, pedicle, transverse process, spinous process, lamina, inferior and superior facets. The vertebral body is the largest part of the vertebrae and the vertebral body is connected to the intervertebral disc. The disc is carrying about 70 percent of the load, while the two facet joints carry the remaining 30 percent. The pedicle connects the posterior elements to the vertebra body and this is a very strong and rigid part of the vertebrae.

Typically the L4 vertebra is the largest vertebrae and the L4 vertebrae is typically located at the same level as the superior part of the ileum crest.

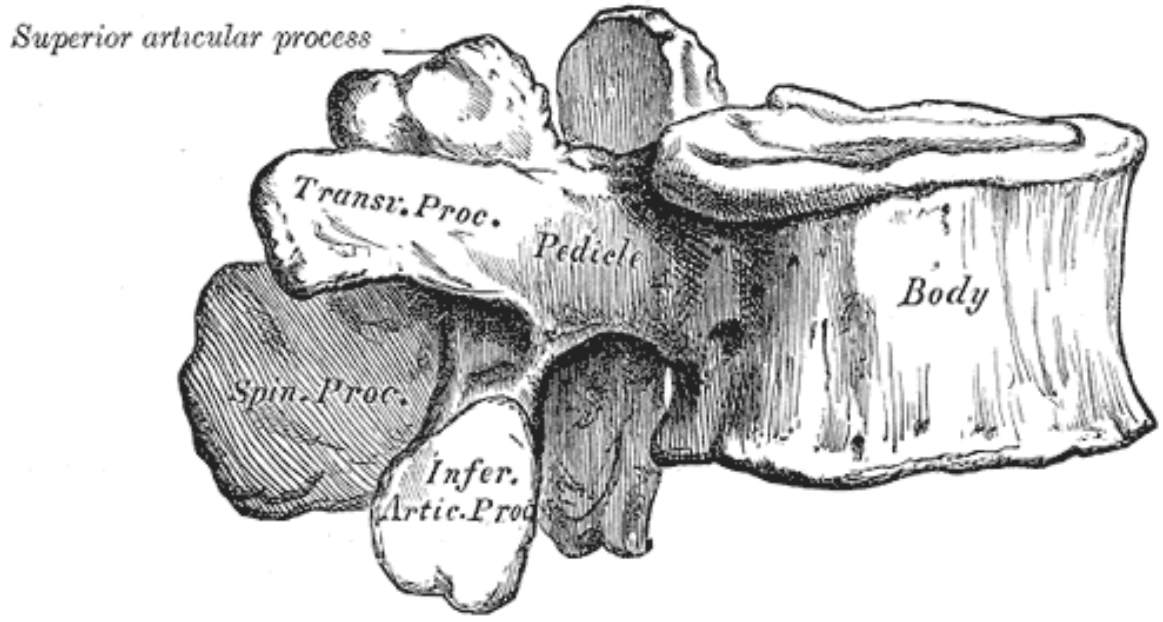

Figure 1-2: A Typical Lumbar Vertebra (Gray's Anatomy)

As seen in figure 1-2, the transverse process is attached to the pedicle and the transverse process is directed in the lateral direction. The facets (labeled as Inferior Articulated Process) are also connected to the pedicle and the facets are directed in the superior and inferior directions. The facet joints consist of the superior facets of one vertebra and the inferior facets of the adjacent vertebrae. These facet joins add stability to the segment and it is also load bearing.

The posterior elements create the spinal canal, which protects the spinal cord.

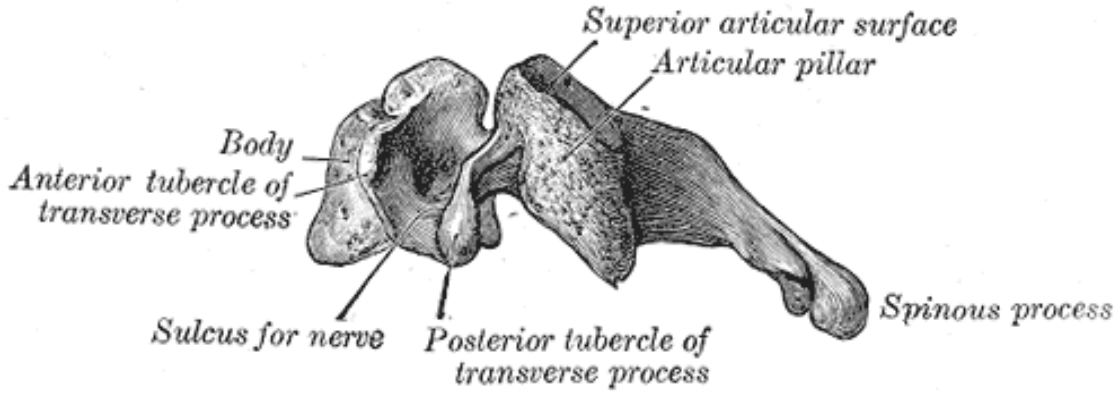

Figure 1-3: A Typical Cervical Vertebra (Gray's Anatomy)

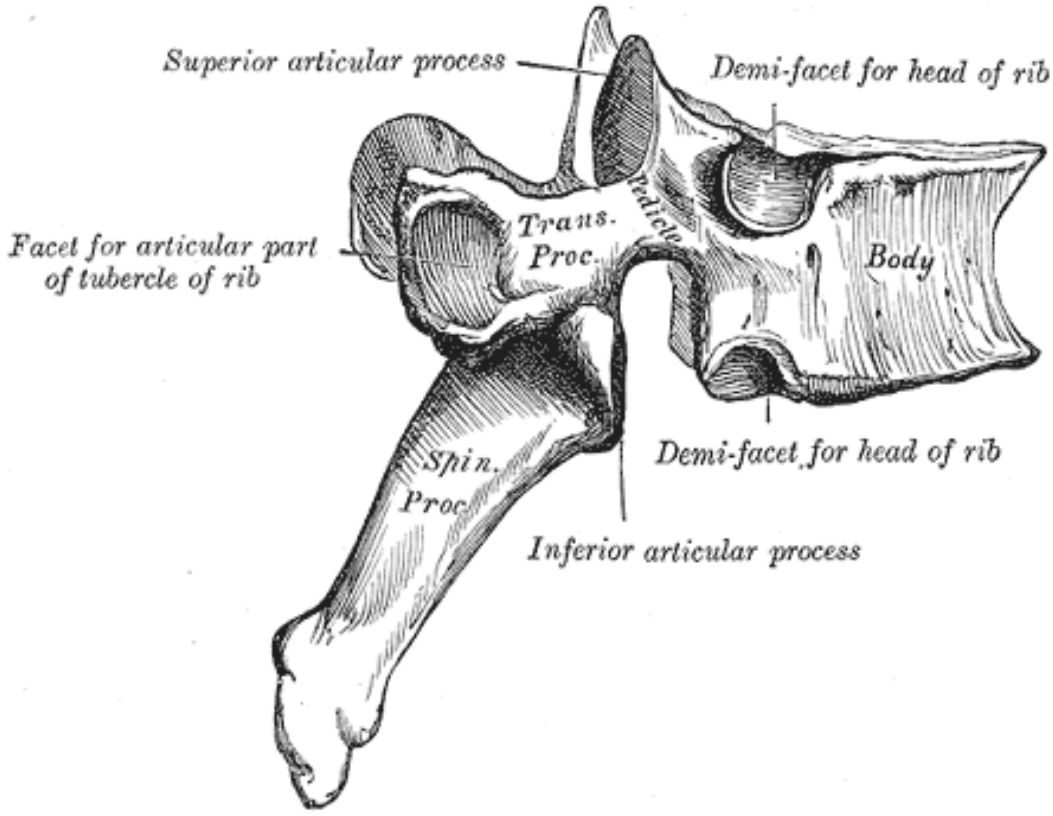

Figure 1-4: A Typical Thoracic Vertebra (Gray's Anatomy)

1.1.1.6 – Cervical Spine

The cervical spine consists of 7 vertebrae (C1-C7), where C1 and C2 are very unique. A typical cervical vertebrae consist of the C1 is also referred to as the atlas and the C2 is referred to as the axis. The atlas has a primary function to support the head and it does not have the body, pedicle, lamina, spinous processes like the vertebral usually do. It consists of two large lateral masses.

The axis is a rigid vertical axis, for rotation of the atlas. The C7 is referred to as the “vertebral prominens” and is the most prominent. It has many characteristics of the thoracic vertebrae.

Cervical spine is the most flexible region (the greatest Range of Motion) of the spine and is also the region with the lowest load bearing capabilities.

1.1.1.7 – Thoracic Spine

The thoracic region has twelve vertebrae. This is also the region where the ribs are connected to the verbal column. The typical thoracic vertebrae are T2-T10 and the an-typical are T1 and T11-T12.

1.1.1.8 – Lumbar Spine

The lumbar region consists of 5 vertebrae and they have wide massive bodies.

The Lumbar region is the section of the spine that has the highest load bearing capabilities, and limited Range of Motion (ROM). The Lumbar region has good ROM in Flexion.

1.1.1.9 – Intervertebral Disc

The intervertebral disc is the flexible portion between the vertebral bodies. This intervertebral disc consists of two major components: nucleus

pulposus and annulus fibrosus. The nucleus pulposus is the center portion of the intervertebral disc and it is an incompressible material. This nucleus pulposus is a gelatinous cushioning part of the intervertebral disc and as the pressure increases, the nucleus bulges and this leads to the disc bulging. The annulus fibrosus are several layers of cartilaginous laminae.

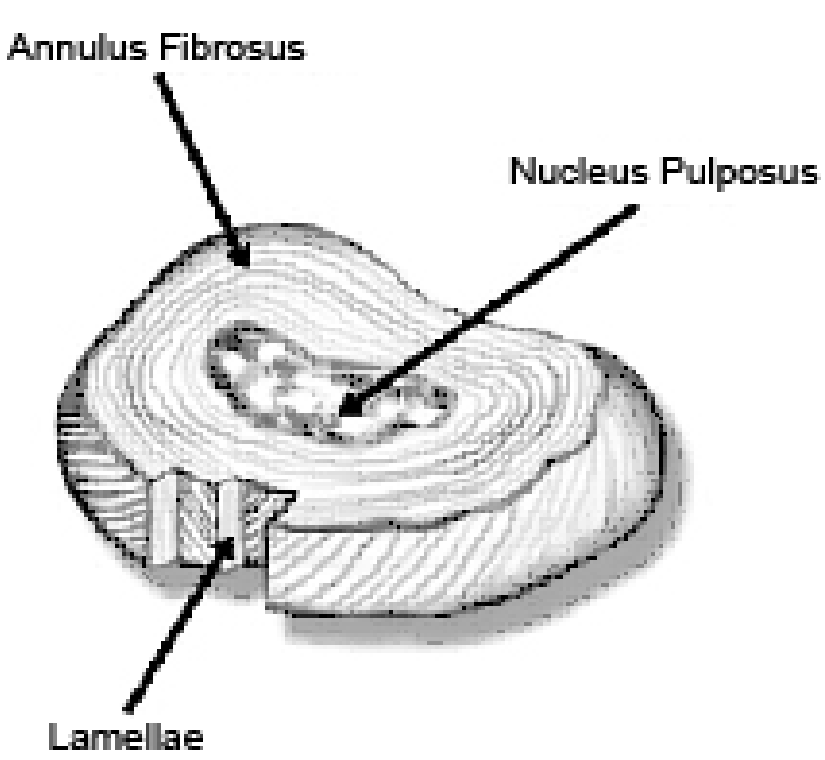

Figure 1-5: A Typical Intervertebral Disc (Gray's Anatomy)

1.2 – Significance

The most common disease, next to the common cold, is Low Back Pain (LBP)[1].

Fusion of adjacent vertebrae is widely used for treating degenerated disc disease, but this procedure does not always alleviate pain[2] and has a degree of comorbidity.[3] Use of conventional (rigid) posterior instrumentation commonly accompanies fusion to prevent motion and aid fusion healing; however, such rigid fixation is believed to accelerate the radiographically observed degeneration of the discs adjacent to the fused segments due to the increased stresses caused by the abrupt stiffness and motion discontinuity.[4-8] As an alternative to rigid fixation, different methods of "soft"[9] or "dynamic"[10-11] stabilization have emerged.[12] Regardless of the name used, these stabilization methods feature some type of less-than-rigid instrumentation design connected to modified pedicle screws for the purpose of gaining more favorable movement and load transmission across non-fused segments. Less than rigid instrumentation seeks to distribute motion rather than eliminate it, and thereby reduce the likelihood of adjacent level disc disease while improving the long term outcome of lumbar fusion procedures.[13]

Treatment of lower back pain can be performed by several different procedures. These procedures typically involve an internal fixation of the lower spine, which is a well established method of reducing lower back pain. To allow fusion, several methods of fixation are used[14-21]. Metal is traditionally used to achieve fixation, which is done by pedicle screw system, translaminar facet screws or facet interference screws[22-27]. Lately, the surgical methods and fixation devices have been rapidly evolving. When internal fixation first began in

the 1940's, Don King developed and implemented a somewhat simple idea for fixation[28]. This method is very similar to what is now referred to as translaminar facet fixation[29-34]. This idea restricts the motion in the facet joint, leading to a fusion of the joint[28,29,35-46].

The idea introduced in the late 1940's was modified by Boucher in 1959 and it is referred to as the "True transfacet" method[36]. This method changes the angle which the screws are inserted, and provides for similar stability and a safer approach. Facet fixation was brought back in 1984 by Magerl, referred to as translaminar transfacet fixation[29]. This is a modification of the original method developed by King[28]. This method is considered easier to perform, more stable and safer than the initial translaminar facet method developed by King[28].

In the 1980's the pedicle screw system became the golden standard, while it might not be the most ergonomically method of fixing the lumbar spine for fusion[24-26]. The pedicle screw system has several disadvantages, but in some cases it is the only option for a successful healing[47-58].

With an increase of medical device development to treat low back pain (LBP), there is also an increasing need for testing of medical devices *In Vitro*[1,59]. Currently, there are no published data that supports the actual forces in the spine during flexion, extension or lateral bending. There are published articles that give *In Vivo* intradiscal pressure measurements for these motions, but there are no correlation performed against *In Vitro* testing results[60-65].

With this increased demand for development and validation of medical devices, the relation to physiological relevance is critical. Currently, there is no physiological rationale for the forces and moments applied during cadaver testing of medical devices. Another increasing problem is the supply of cadaver tissue and mathematical models are increasing in popularity. By collecting scientific data, this data can be used to validate mathematical models.

1.3 – Objective

There are three main objectives to this dissertation. As earlier stated, these are both analytical and experimental. The analytical section is accomplished by the use of a finite element model to calculate and compare the stresses in the adjacent level disc that are induced by conventional and “dynamic” posterior lumbar fusion instrumentation. The hypothesis of this particular study was validation of the incidence of adjacent level disc disease in the lumbosacral spine will be decreased with the use of semi-rigid rods.

The second section of this dissertation contains the experimental evaluation. Here, a comparison of the biomechanical properties of a facet fusion allograft *In Vitro* was performed. The hypothesis is to investigate that the stiffness and stability of spine will increase by implanting facet fusion allograft.

The last objective of this dissertation was to find relationship between *In Vivo* and *In Vitro* spinal mechanical loads. This was done by comparing the

published *In Vivo* intradiscal pressures to *In Vitro* intradiscal pressures and evaluate the effects of moments applied *In Vitro*.

1.4 – Outline of the Dissertation

The remaining of the dissertation is organized as follows. In Chapter 2, the general materials and methods of the analytical and experimental work is described. Application specifics are explained in the respective chapters. Chapter 3 describes the analytical section of the dissertation, which contains a three dimensional finite elements study of the lumbar spine.

The experimental work is shown in chapter 4 and 5. In chapter 4, a facet fusion allograft is investigated. *In Vitro* Intradiscal pressure measurements are conducted in chapter 5 and compared to published *In Vivo* data. This comparison shows how much mechanical load is acting on the spine.

Chapter 6 summarizes the dissertation research, outlines the contributions and provides some recommendations for future work.

CHAPTER 2 – MATERIALS AND METHODS

2.1 – Analytical

Engineering is in general problem solving by using mathematical models of physical situations. In traditional engineering, finite element method has been used extensively and is increasing in popularity in the medical field. The mathematical models are differential equations developed to solve the boundary and initial conditions. By applying fundamental laws and principles, these differential equations are derived based upon mass, force or energy.

There are two methods; Force method, where the forces are unknown and displacement method, where displacements are unknown. There are limitations to the force method, so the current use in finite element method is the displacement method.

The governing equation for finite element method is a relation between the force, displacement and the stiffness. Seen below, is a sample of a two dimensional finite element method equation.

$$\begin{bmatrix} \vec{F}_{1x} \\ \vec{F}_{2x} \end{bmatrix} = \begin{bmatrix} \vec{k}_{11}\vec{k}_{12} \\ \vec{k}_{21}\vec{k}_{22} \end{bmatrix} \begin{bmatrix} \vec{d}_{1x} \\ \vec{d}_{2x} \end{bmatrix} \qquad \text{(Equation 2-1)}$$

This equation shows the force (F), the displacement (d) and the stiffness (k). There are generally eight steps to solving a problem with finite element method. The first step is to select an element. Depending on the problem, a one, two or three dimensional element can be used. A first or second order element, as well as the shape of the element must be used. Second order elements have more nodes, and gives better accuracy. The next step is to choose the displacement functions as shown below.

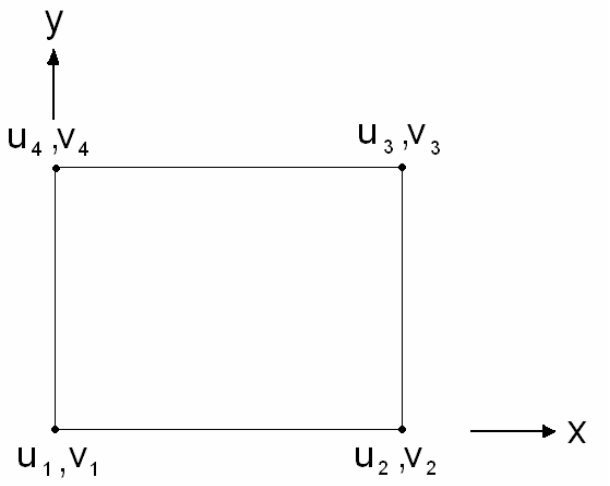

Figure 2-1: Displacement Function for Finite Element Method

Next, a definition of stress/strain and strain/displacement relationship is needed. This is done by applying boundary conditions. From this, the element stiffness matrix can be defined and the global equations can be assembled. With the global equations, a solution for displacement can be found. The displacements will be used to find the stress and the strain and the results are interpreted. The specifics for this particular study, is explained in detail later on in the dissertation.

2.2 – Experimental

2.2.1 - Biomechanical Testing

A nondestructive spine biomechanics test setup was used to find the biomechanical properties. This particular setup is based on an axial servo-hydraulic materials testing system (MTS Systems Inc., 858 Bionix II, Eden Prairie, MN) and is modified to allow bending as well as axial rotation. Axial compression is integrated in the MTS 858 Bionix II and the load is measured by the use of a load cell. The MTS 858 Bionix II with the modifications can be seen below in figure 2-2.

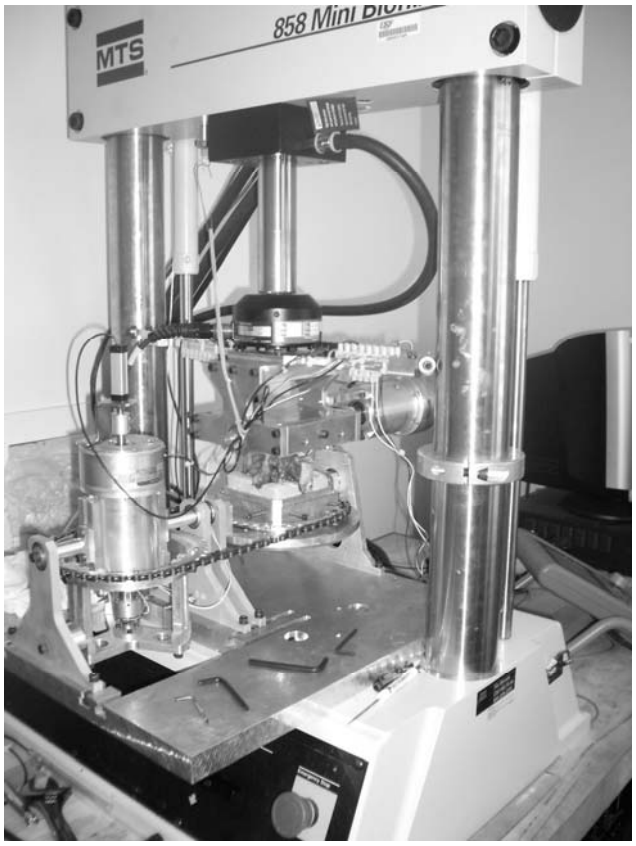

Figure 2-2: The MTS 858 Bionix II Spine Tester at University of South Florida

The load cell is an electronic device (transducer) that is used to find the axial force applied. The load cell measures strain, by the use of a Wheatstone bridge strain gage. Since the load cell measures dynamic load, there is a constant feed back and error correction process. This will generally cause the signal to oscillate, but by the use of a controller system, this oscillating effect is minimized. The control systems consist of an actuator that actively dampens the effect of the oscillation. This method offers great performance, but the process is complex and costly.

These load cells are calibrated on site by the manufacturer. The general method of calibration is simply to apply a known force by the help of gravity. Since the applied static force is known, the load cell can be calibrated accordingly. This procedure is done with a series of different loads, and a calibration equation is developed. The load cell has an accuracy of 0.13% error for force measurements and 0.10% for displacement measurements.

Figure 2-3: MTS Force Transducer Used on the Experimental Apparatus

The displacement is measured by a linear variable differential transformer. The linear variable transformer measures the absolute position by using the magnetostrictive measuring principle developed by J. Tellermann. This method uses magnetic fields and waveguides to determine the distance

the ultrasonic wave travels. These linear variable differential transformers are calibrated by the manufacturer and have an accuracy of 0.01%

The torsion and bending motions are measured by linear variable differential transformers. The linear variable transformers record the angular displacement and an approximate error of 1%. The angular displacement is calibrated by positioning the device in series of different known angles and finding the proper gain settings for the particular device.

The torque is measured by an electronic device (transducer) that is called a torque cell. In a very similar manner to the load cell, the torque cell measures strain, by the use of a Wheatstone bridge strain gage. Since the torque cell measures dynamic load, there is a constant feed back and error correction process. This will generally cause the signal to oscillate, but by the use of a controller system, this oscillating effect is minimized. The control systems consist of an actuator that actively dampens the effect of the oscillation. This method offers great performance, but the process is complex and costly. The torque cells are calibrated by inputting a linear series of known torque to find the proper gain. The accuracy of these torque cells are approximately 1%.

The axial force and axial displacement are continuously recorded and can be used to interpret the axial stiffness of the specimen. Axial torsion is measured by fixing one end of the specimen and applying an axial torque on the other end of the specimen. By measuring the torque and the axial rotational

angle, the rotational resistance can be calculated. The bending consists of a superior and inferior moment and an equal, but opposite bending moment is applies at both ends. This allows for pure bending moment and no shear is present. The bending moment and the angle are recorded throughout the cycle for an accurate measurement of the bending stiffness. This bending moment is used to measure flexion/extension and by turning the specimen 90 degrees, it will measure lateral bending.

2.2.2 – Intradiscal Pressure Measurements

The intradiscal pressure measurements were performed by inserting a cannulated needle into the center of the nucleus propulsus[66,67]. The nucleus propulsus is uniformly hydro static and gives a comparable reading through out the majority of the nucleus. An approximation of the center of the nucleus was done by measuring the radiographic images. Once the center of the nucleus was found, a calibrated pressure probe (OrthoAR Model No: 0571521-57, Medical Measurements Inc., Hackensack, NJ) was inserted through the cannulated needle and the pressure sensor was exposed to the hydrostatic pressure of the nucleus propulsus.

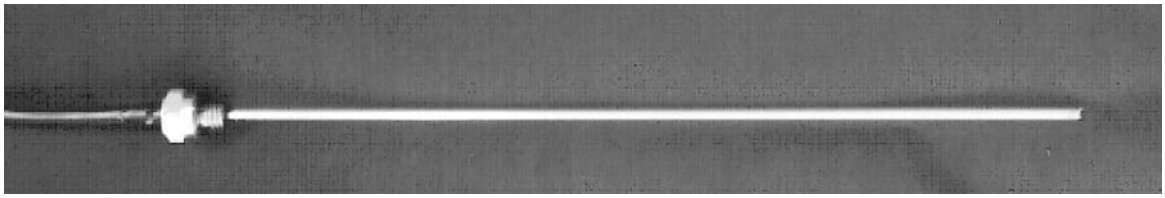

Figure 2-4: Pressure Probe Made by OrthoAR

The pressure probe is a Piezoresistance of semiconductor device, based on a microelectromechanical system (MEMS) Wheatstone bridge strain gage. The strain gage changes the resistance accordingly to the strains in the pressure probe. The output voltage is changing as a result of the change in resistance, and the voltages are recorded and interpreted by the MTS software.

The pressure probe is calibrated by using nitrogen pressure. A known pressure of nitrogen is released into a sealed container, where the pressure probe is inserted. This procedure is done with small increments and a graph of the known pressure can be plotted against the change of resistance in the strain gage in the tip of the pressure probe. The gain on the pressure probe can be adjusted accordingly and verification is done. The pressure probe has a certified sensitivity of 0.496 μV/V-kPa at a pressure of 2 MPa with an error of 0.3% at 1 MPa according to National Bureau of Standards. The pressure sensor was horizontal oriented, as there is no significant difference in orientation[68].

2.2.3 – Human Cadaver Tissue and Fixation

The human cadaver tissue is supplied by National Disease Research Interchange to be used for research only. This tissue is harvested at the hospital within 12 hours and stored at -80 degrees Celsius. The tissue has passed all the serologic testing before shipping, while care must still be taken. The tissue is inspected upon arrival and stored at -80 degrees until use. Tissue is handled professionally, with respect, care and disposed in a proper manner.

The lumbar spine segments are disarticulated and potted into 4” x 4” aluminum fixtures by the use of polyester resin and anchors. Figure 2-5 below is a sample image of a FSU potted on both sides and securely fastened in the fixture.

Figure 2-5: A FSU Potted on Both Sides

An important aspect of potting is not to disturb the disc space. A digital Faxatron (Model No: MX-20, Wheeling, Illinois) is used to capture an X-Ray to verify that the disc space is not violated. Figure 2-6 below show a sample X-Ray of the potted FSU, and there are no objects in the disc space to alter the biomechanical behavior.

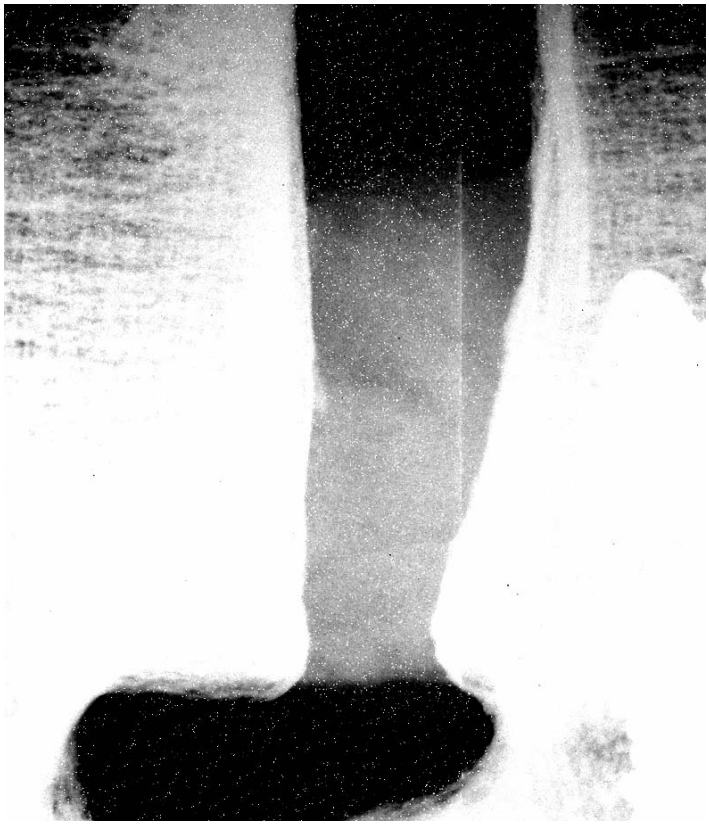

Figure 2-6: X-Ray Image of a Potted Specimen, with No Anchors in the Disc Space

Once the potting is performed, the FSU are covered with gauss and sprayed with saline solution. When the specimens are not in use, they are stored at +4 degrees Celsius to minimize tissue degradation.

CHAPTER 3 – FINITE ELEMENT ANALYSIS OF DYNAMIC INSTRUMENTATION DEMONSTRATES STRESS REDUCTION IN ADJACENT LEVEL DISCS

3.1 – Introduction

Conventional fusion instrumentation is believed to accelerate the degeneration of adjacent discs due to the increased stresses caused by motion discontinuity. Fusion instrumentation that employs reduced rod stiffness and increased axial motion, i.e. “dynamic” instrumentation, may partially alleviate this problem, but the effects of this instrumentation on the stresses in the adjacent disc are unknown. The objective of this study was to use a finite element model to calculate and compare the stresses in the adjacent level disc that are induced by conventional and “dynamic” posterior lumbar fusion instrumentation.

The efficacy of dynamic stabilization remains controversial, and is therefore a suitable topic for continuing investigation[2,70-73]. Although several clinical outcome studies describe preliminary results obtained from the use of dynamic stabilization[3,4,12,23,26], these studies lack a randomized controlled design, a statistically adequate sample size, or long-term follow-up data that

would enable the clinical efficacy of these methods to be properly evaluated[10]. Early data suggests that the results are at least no worse than those observed from conventional rigid instrumentation[2]. Information is also lacking from a scientific perspective because dynamic stabilization methods have largely been developed based on clinical suggestions instead of quantitative engineering design efforts, and thus the biomechanics of these methods remain relatively unstudied.

Therefore, the purpose of the present study was to: 1) quantify the biomechanics of rigid and one other specific type of dynamic instrumentation when biomechanically tested in a simulated laboratory model, 2) use these data in a finite element model of a fused and fixed lumbar spine to calculate the flexion-induced peak stresses in the adjacent level discs, and 3) compare these results to determine if a biomechanical basis exists for believing that the reduced stiffness and increased axial motion conferred by dynamic instrumentation can alter the stresses in adjacent level discs.

3.2 – Materials and Methods

3.2.1 – Study Design

This laboratory study, performed at University of Kentucky, used both standardized compressive testing of dynamic instrumentation on an established lumbar spinal segment model, as well as a finite element modeling technique

which enabled quantification of the stresses induced in an established model of lumbar spinal discs[74] as a function of instrumentation design (rigid or conventional vs. dynamic). This experimental design, i.e., stiffness testing followed by finite element analyses, is consistent with prior studies[75-76].

3.2.2 – Finite Element Modeling

A three dimensional finite element model of the lumbar spine (L1-L5 including discs) was developed by first obtaining a validated finite element mesh[74] for the L3-L5 spine section. (Figure 3-1)

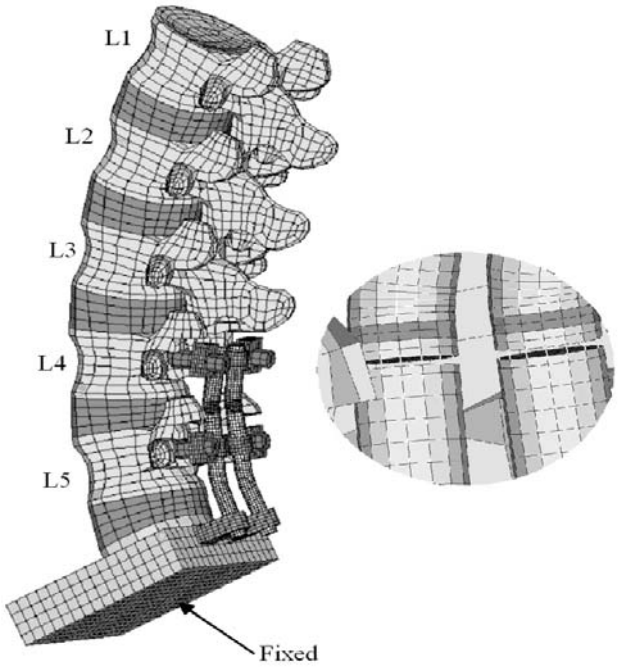

Figure 3-1: Isometric View of the Finite Element Mesh of the Lumbar Spine and the Semi-Rigid Rod

Isometric view of the finite element mesh adapted from a model created and validated by Smit et al from which a model of the lumbar spine was used and to which the semi-rigid instrumentation was applied.

The geometry had been developed based on a series of computed tomography scans of the L4 vertebra of a 44 year male with no pathologies[74]. The L4 mesh was then replicated to model the other lumbar spine vertebrae. Note that this validated model of L1 – L5, previously developed by Smit et al., consists of a series of five dimensionally equivalent L4 vertebrae. This resulting mesh of L1-L5 vertebrae was positioned such that the angle between the inferior surface of L2 and the superior surface of L5 was 40 degrees. This model consisted of a fused (totally rigid) L5-S1 segment and a L4-L5 segment that was modeled to imitate fixation with either rigid or dynamic instrumentation. The dimensions for the instrumentation used in this model were obtained from direct measurement of exemplar instrumentation (Isobar TTL, Scient'X USA Inc, Maitland, FL, USA). The fused segments between L5-S1 were modeled by specifying the material properties of the L5-S1 disc to be the same as those of cortical bone. Adjacent pairs of vertebrae were connected by intervertebral discs that were modeled by a nucleus in the center surrounded by 3-4 rings of annulus fibrosus. The nucleus typically occupies about 30-50% of the area of the disc; therefore the fraction used for the nucleus in the model obtained was 43%[77].(Figure 3-2)

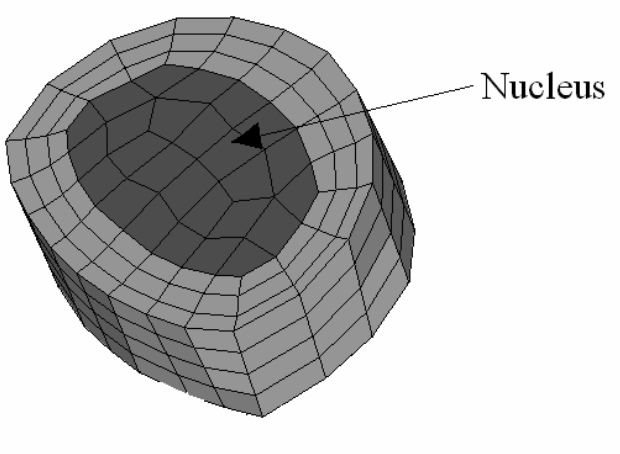

Figure 3-2: Isometric View of an Intervertebral Disc

Isometric view of an intervertebral disc used in the model. Model shows the annulus fibrosis (outer three layers of mesh elements) and the nucleus pulposis (darker inner mesh elements)

The entire finite element model contained 18,128 three-dimensional 8-node linear brick elements.

Loading of the model was accomplished by combined flexion or extension plus axial loading. The axial load of 400 N was applied as a "follower" load thereby allowing the axial load to follow the motion of the spine. The model simulated forward flexion at discrete angular increments of 15°, 30° and 45° and a backwards extension of 15° by applying relative angular

displacements between L1-L2, L2-L3, and L3-L4 segments, respectively, based upon values equal to those obtained from a normal spine during forward flexion and backward extensions[78].

The damper of the dynamic instrumentation, located between the instrumented L5 and L4 vertebrae, permitted the upper segment of the fixation rod to have a reduced stiffness and a limited amount of axial micromotion. These two features of this damper mechanism were modeled by employing a softer segment (having variable stiffness values, all of which were less than those of titanium alloy) placed in series with an axial motion connector (which allowed axial motion only). (Figure 3-3)

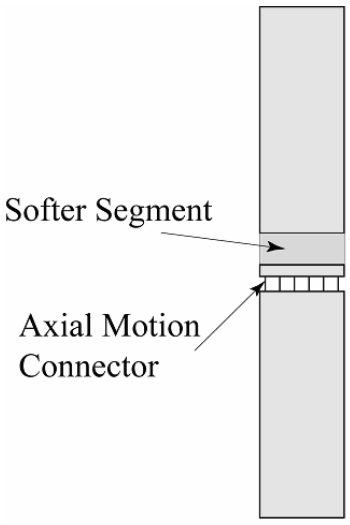

Figure 3-3: The Damper Model of the Dynamic Instrumentation

Expanded schematic illustration of the mechanical components of the damper element of the dynamic instrumentation component (shown in Figure 3-1).

Two parameters, R and G, were used in this model to quantify the reduced stiffness and the axial micromotion of the damper mechanism, respectively. Note that the damper is an integral component of the TTL device which is responsible for these two features. The parameter,

$$R=K_{rigid}/K_{dynamic} \qquad \text{(Equation 3-1)}$$

was used to quantify the reduced stiffness of the damper. (This dimensionless stiffness ratio quantified how much stiffer the rigid instrumentation was relative to the dynamic instrumentation. The K_{rigid} term of equation [3-1] represents the elastic stiffness of the rigid instrumentation, while the $K_{dynamic}$ term represents the elastic stiffness of the dynamic instrumentation. Values for K_{rigid} and $K_{dynamic}$ were obtained from the material properties of titanium alloy and the variable reduced stiffness material comprising the softer segment. The G parameter was defined as the maximum axial motion allowed by the damper mechanism. To study the effects of axial motion on the resulting pressures inside the disc, five discrete maximum allowable axial displacements (0 to 0.8 mm in 0.2 mm increments) were used in the model. Changes to both R and G permit the changes in pressure within the disc to be quantified as a result of varying

instrumentation elastic stiffness and axial micromotion. Before reaching the maximum axial motion, the damper also functioned as an axial spring with a stiffness of 175 KN/m (calculated from the product manual accompanying the Isobar TTL instrumentation).

The inferior portion of the sacrum was modeled as a block and the lower surface of the block was considered fixed. A static compressive ("follower") load of 400 N was axially applied to the superior surface of the L1 vertebra and this load was maintained perpendicular to the superior surface of the L1 segment throughout axial load induced deformation. All components in the assembly shown (Figure 3-1) were modeled by using linear elastic materials. The material properties assigned to these components[74,78] in the finite element model are shown (Table 3-1).

Material properties obtained from sources listed and used in the finite element model. Units of Young's Modulus are gigaPascals; Poisson's ratio is dimensionless.

Table 3-1: Material Properties

Material	Young's Modulus, GPa	Poisson's Ratio
Cortical Bone	12	0.3
Cancellous Bone	3	0.2
Fibrous	0.03	0.45
Nucleus	0.001	0.49
Steel	190	0.3
Titanium	116	0.33

Peak stress values in the disc, as well as the areas of the 2D projections of the 3D volumes of disc tissue exposed to > 80% of peak stress volumes, were calculated for varying values of R and G by using commercially available finite element analysis software (ABAQUS/Standard, ABAQUS Inc., Pawtucket, RI).

3.3 – Results

The experimental testing performed at University of Kentucky, showed mean value of the elastic stiffness (axial load divided by actuator displacement)

of the rigid instrumentation was 21,960 ± 8,034 N/mm, while the mean elastic stiffness of the dynamic instrumentation was less than one-third this value (p = 0.01), i.e., 6,169 ± 1,298 N/mm. Using these data, the resulting R and G values for the rigid instrumentation were 1 ("control" stiffness value) and 0 (meaning no axial micromotion – obtained from the manufacturer), respectively, whereas the R and G values for the dynamic instrumentation were 3.6 and 0.4 mm, respectively. Other values for R and G were also used in the model calculations to compute the effect of alternative values for elastic stiffness and axial micromotion. (Tables 3-2 & 3-3).

Table entries (italicized values) are the peak stresses (units of gigaPascals) induced in the L3 – L4 disc superior to the dynamic instrumentation component as calculated from the finite element model as a function of: 1) flexion (+ value)/extension (- value) angle (extreme left column), 2) dimensionless stiffness ratio R (second column from left), and 3) axial motion parameter G (column headings, units of mm).

Table 3-2: Peak Calculated Stress (MPa) in the L3-L4 Disc

Angle, degrees	G(mm) / R (ratio)	0.0	0.2	0.4	0.6	0.8
45	1	*7.7096*	*7.5364*	*7.3715*	*7.2067*	*7.0422*
	3.6	*7.6376*	*7.4578*	*7.2866*	*7.1157*	*6.9453*
	10	*7.5644*	*7.3867*	*7.2174*	*7.0485*	*6.8800*
	44	*7.3416*				
30	1	*5.0483*	*4.8767*	*4.7133*	*4.5503*	*4.3882*
	3.6	*4.9999*	*4.8211*	*4.6511*	*4.4814*	*4.3123*
	10	*4.9524*	*4.7754*	*4.6069*	*4.4388*	*4.2712*
	44	*4.8044*				
15	1	*2.4776*	*2.3078*	*2.1472*	*2.0859*	*2.0859*
	3.6	*2.4532*	*2.2759*	*2.1077*	*1.9404*	*1.9101*
	10	*2.4303*	*2.2542*	*2.0870*	*1.9209*	*1.8515*
	44	*2.3569*				
-15	1	*4.2420*	*4.0428*	*3.8508*	*3.8508*	*3.8508*
	3.6	*4.2348*	*4.0251*	*3.8066*	*3.7431*	*3.7431*
	10	*4.2215*	*4.0126*	*3.7947*	*3.7093*	*3.7093*
	44	*4.2085*				

Table entries (italicized values) are the peak stresses (units of gigaPascals) induced in the L4 – L5 disc spanned by the dynamic instrumentation component as calculated from the finite element model as a function of: 1) flexion (+ value)/extension (- value) angle (extreme left column), 2) dimensionless stiffness ratio R (second column from left), and 3) axial motion parameter G (column headings, units of mm).

Table 3-3: Peak Calculated Stress (MPa) in the L4 – L5 Disc

Angle, degrees	G(mm) / R (ratio)	0.0	0.2	0.4	0.6	0.8
45	1	2.5972	2.7377	2.8713	3.0043	3.1369
	3.6	2.7141	2.8765	3.0317	3.1872	3.3429
	10	2.7601	2.9242	3.0812	3.2386	3.3964
	44	2.9633				
30	1	1.7221	1.8579	1.9873	2.1165	2.2448
	3.6	1.8010	1.9591	2.1105	2.2624	2.4147
	10	1.8309	1.9912	2.1448	2.2990	2.4537
	44	1.9626				
15	1	0.8522	0.9844	1.1106	1.1588	1.1588
	3.6	0.8921	1.0470	1.1955	1.3443	1.3713
	10	0.9067	1.0642	1.2153	1.3667	1.4300
	44	0.9717				
-15	1	0.4319	0.8208	1.2029	1.2029	1.2029
	3.6	0.4803	0.8214	1.1828	1.2882	1.2882
	10	0.5368	0.8616	1.2055	1.3410	1.3410
	44	0.8796				

Calculated values are shown for the peak von Mises stresses induced in the L3-L4 disc for the 400 N axial load applied with each of the two instrumentation designs at each of the four flexion/extension positions (15°, 30° and 45° flexion and 15° extension) and for varying values of R and G (Table 3-2). The data showed that the use of dynamic instrumentation was associated with a 5.5% reduction in peak stress for the L3-L4 disc and a 16.7% increase in peak stress for the L4-L5 disc compared to the rigid instrumentation at 45° of flexion. It was also observed that, by maintaining the G value at 0.0 (allowing no axial micromotion) but allowing the stiffness of the proximal segment of the dynamic instrumentation to decrease, caused a reduction in the peak stress in the L3-L4 disc by approximately 1-2%. Alternatively, maintaining the same stiffness of this proximal segment as is found in the rigid case, i.e., maintaining the R-value at 1, but increasing the axial micromotion, i.e., increasing the G-value, results in reducing the peak stress in the L3-L4 disc by approximately 8-9%. Thus, increasing the G-parameter (specifically, increasing axial micromotion) was shown to be more effective in reducing the peak stress in the L3-L4 disc than was decreasing the R-parameter (specifically, decreasing the rod stiffness). The effects noted above were also observed at 15° and 30° of flexion as well as at 15° of extension, but less prominently (Figure 3-4).

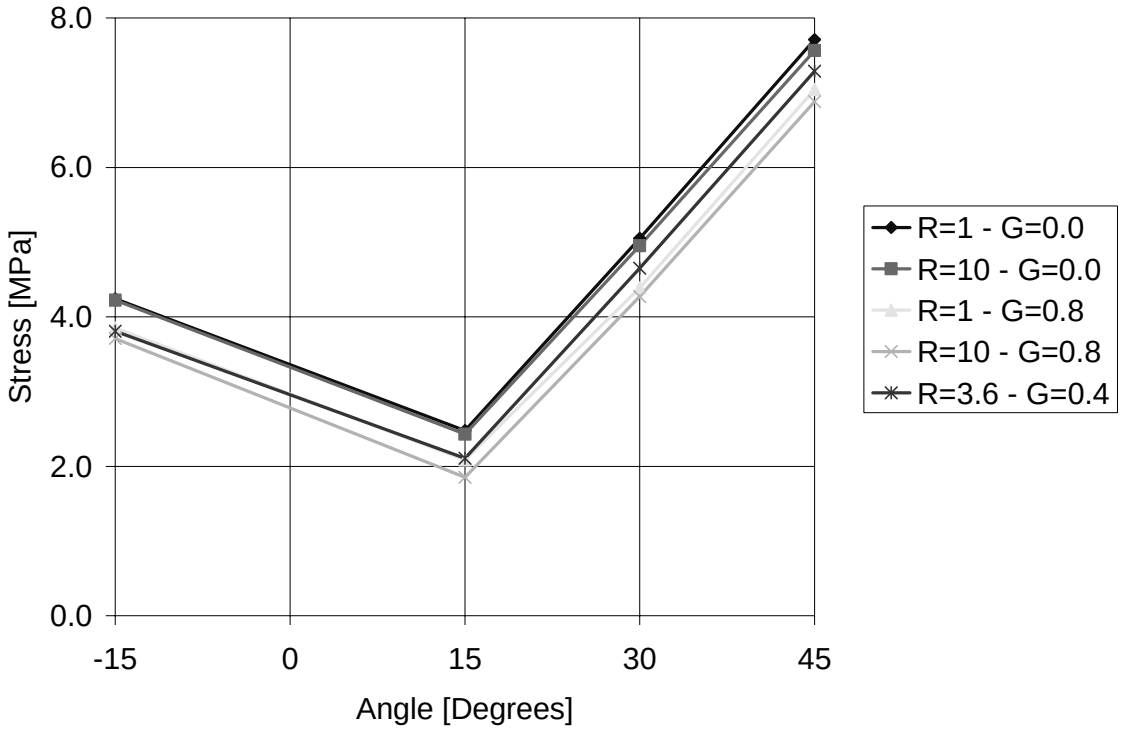

Figure 3-4: Comparison of Stress in L3-L4 with Different Variables for R and G

Representative values for the calculated stresses induced in the L3-L4 disc as function of one of four different flexion/extension angles (abscissa) and for varying indicated (color-coded values of relative stiffness (R-parameter values) and axial motion (G-parameter values).

Note that the minimal value for peak stress in the L3-L4 disc in the 45° flexion case was achieved for R and G values of 10 and 0.8 mm, respectively.

To graphically visualize the stress reduction caused by reduced stiffness and increased axial micromotion associated with dynamic instrumentation, the

stress levels in the L3-L4 disc located above the rigid instrumentation were contrasted with those of the same disc located above dynamic instrumentation which have the “optimal” dynamic parameters (R=10, G=0.8 mm) noted. (Figure 3-5).

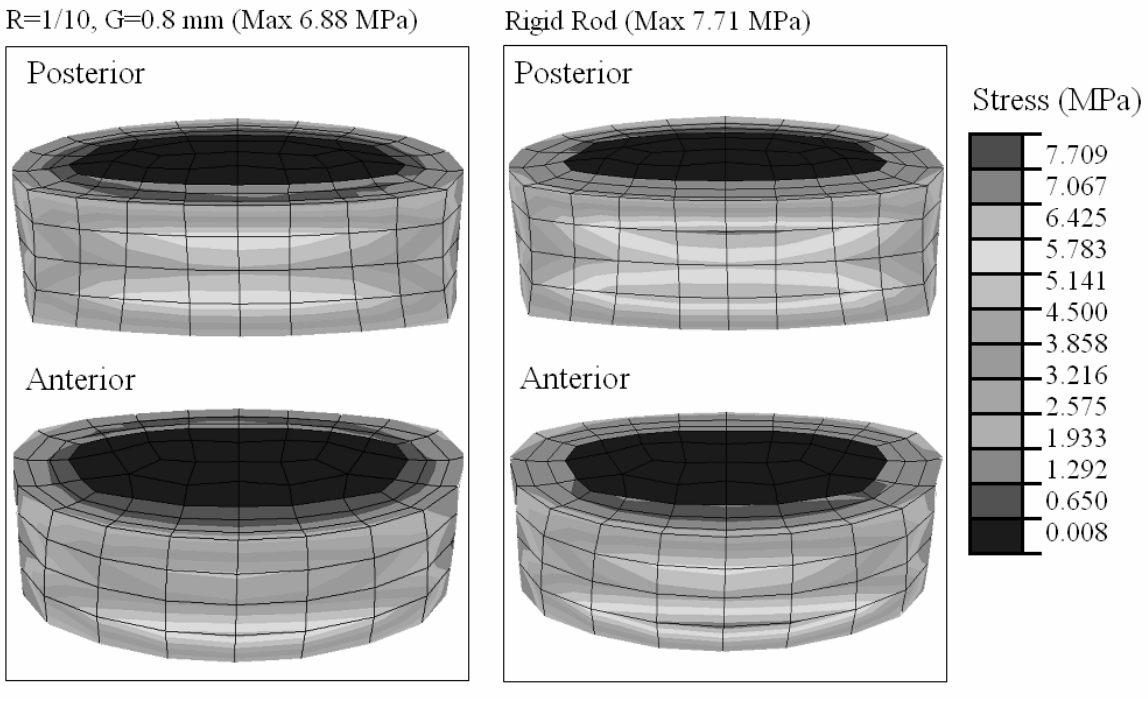

Figure 3-5: Stress Distribution of L3-L4 at 45˚ Flexion.

Anterior and posterior views of calculated stress distribution in the L3-L4 disc at a 45˚ flexion angle for discs associated with rigid instrumentation (right side) and “dynamic” (left side) instrumentation (1/10 stiffness, i.e., R = 0.1) for 0.8 mm axial motion.

A representation of the peak stresses for the extreme motions are shown below in figures 3-5, 3-6 and 3-7. These cases are all achieved with R and G values of 10 and 0.8 mm, respectively. The remaining representations are shown in Appendix A.

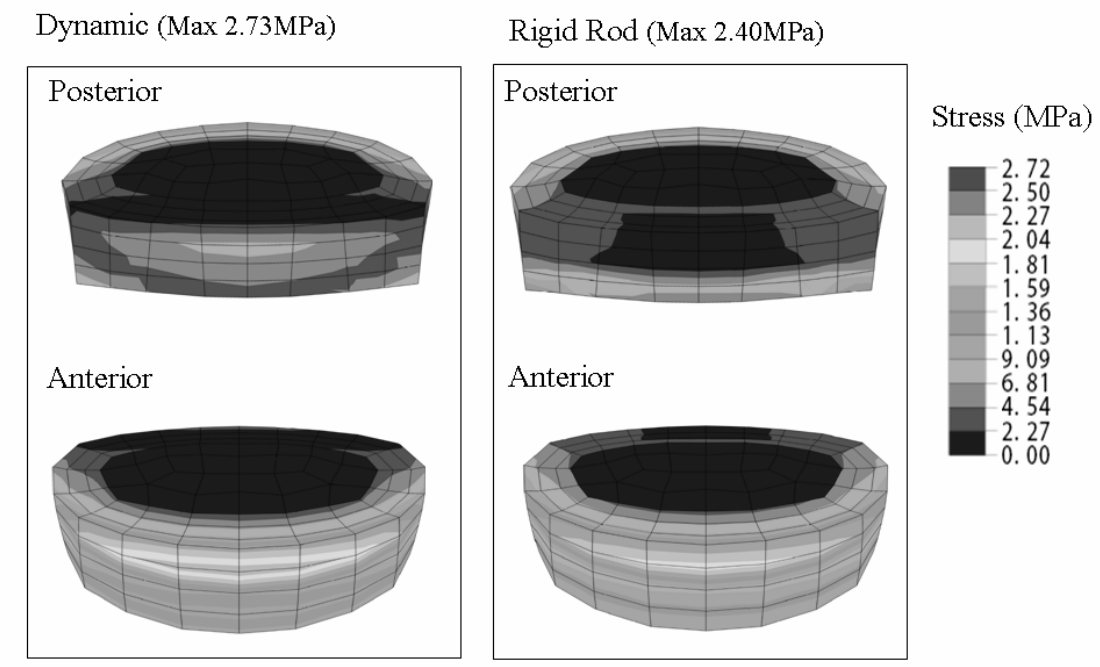

Figure 3-6: Stress Distribution of L4-L5 Disk at 45˚ Flexion

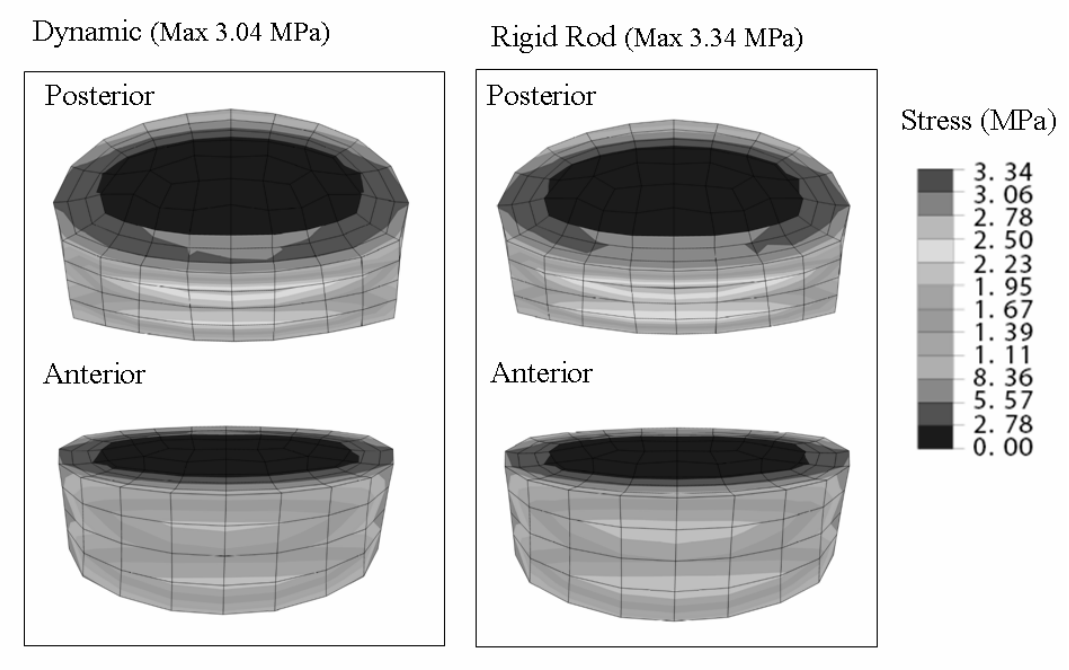

Figure 3-7: Stress Distribution of L3-L4 Disk at 15˚ Extension

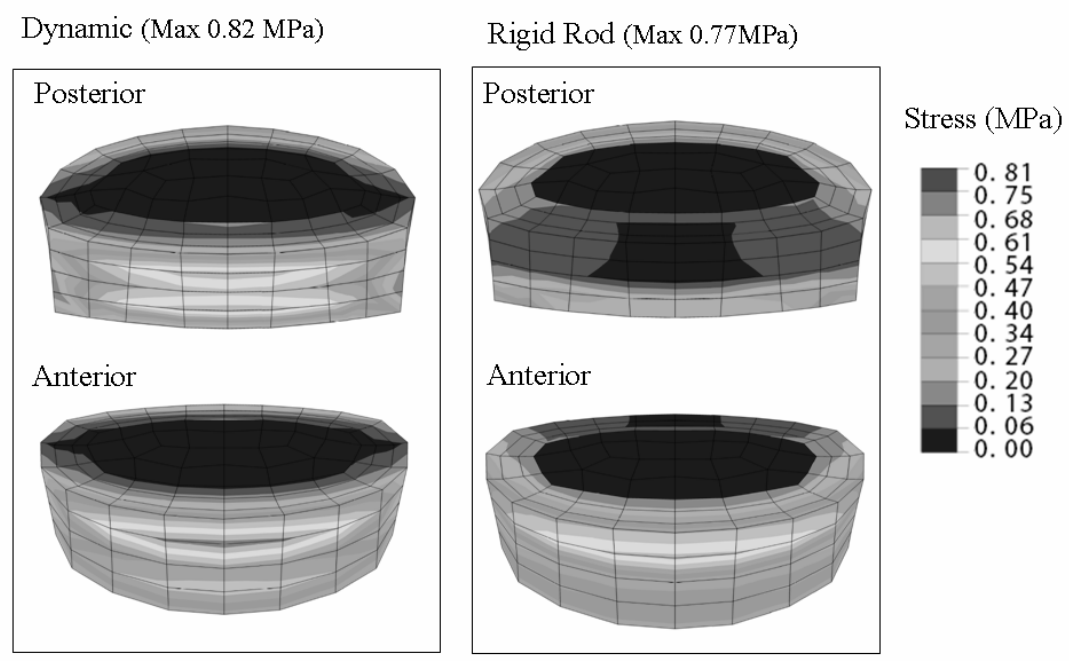

Figure 3-8: Stress Distribution of L4-L5 Disk at 15˚ Extension

Note from these stress contours that the volume of L3-L4 disc tissue located above the dynamic instrumentation that was exposed to stresses of 6.17 MPa or greater was 47% less than the volume of L3-L4 disc tissue located above the rigid instrumentation that was exposed to stresses of 6.17 MPa or greater. The stress value 6.17 MPa was 80% of the peak stress in the L3-L4 disc located above the rigid instrumentation when calculated at 45° of flexion.

3.4 – Discussion

Reduced stiffness and increased axial motion of dynamic posterior lumbar spinal fixation instrumentation resulted in both lower peak stresses and smaller volumes of tissue exposed to high amplitude stresses in simulated adjacent level discs. While the stress reduction effect was small (~10% cumulatively for a single forward flexion), this is important because this benefit will be repeated over many loading cycles (1 – 10 million/year). Classic material fatigue studies show that small reductions in peak load amplitude produce substantial increases in material longevity, and this finding is substantiated by analogous studies conducted in cadaveric lumbar vertebrae[70]. Although the reduced stiffness and increased axial motion also increased the peak stress in the L4-L5 disc by up to 28%, this load increase needs to be considered in light of the peak stress amplitude in the L4-L5 disc which was 2 to 3 times less than that in the adjacent L3-L4 disc. The reduced stiffness and increased axial motion of dynamic instrumentation also allows some rotation of

the L4 vertebra with respect to L5. This rotation is not permitted by rigid instrumentation designs. To achieve the same overall level of flexion when both types of devices are used, the L3-L4 disc experiences smaller rotation demands when this type of dynamic instrumentation is used. This reduced rotation then leads to a corresponding stress reduction in this disc.

There are only a few published studies that are reasonably comparable to the present study. Three of these used cadaveric spinal segments that were mechanically tested *In Vitro* in conjunction with another type (Dynesis) of dynamic instrumentation. All showed that this type of dynamic instrumentation can favorably alter load transmission and movement yet can also provide adequate stability. None of these studies quantified the changes in pressure within the disc that remain at the basis of adjacent segment degeneration[79-81]. Another study used computational models to compare materials selection, but not device design. This study also focused on overall mechanical stability and load transmission rather than pressures within the disc[76]. A fifth study used a finite element method to compute pressures within adjacent discs, but did not study the effects of dynamic instrumentation[82]. The one study most closely similar to that done presently[83] also used a finite element model of the lumbar discs, but concluded that dynamic instrumentation does not alter pressures within the discs. The reason for this disparity in findings may be reflective of the mechanical performance differences between the Isobar system (present study) and the Dynesis system (Zander et al. study).

It is important to note that dynamic instrumentation also permits axial distraction, which in turn changes the center of rotation. Consider the two instrumented segments, A and B. (Figure 3-9a).

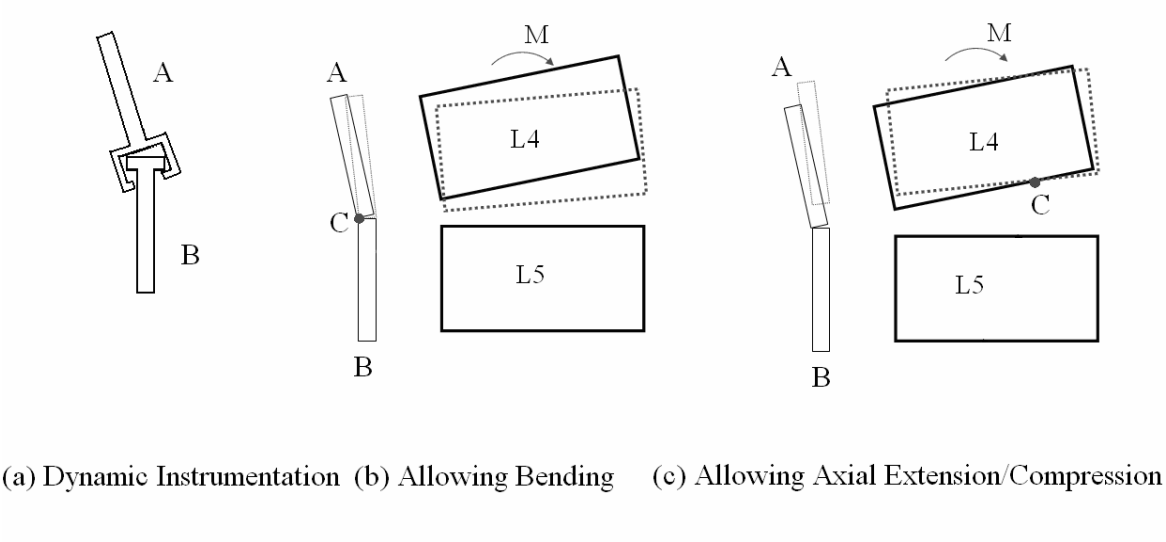

Figure 3-9: Two Approaches to Generate 2˚ of Rotation

Saggital view of a schematic illustration of the damper mechanism that shows two approaches regarding how rotation can be obtained for instrumentation that allows "dynamic" motion (a): (b) pure bending only with no axial motion – notice the location of the Center of Rotation (COR), or (c) bending with axial compression/extension – note the altered (more physiological) location of the Center of Rotation.

If axial distraction (i.e., increase of the inter pedicular distance) is permitted, then the center of rotation shifts and falls within the L4-L5 disc and not on the posterior side of the posterior lateral ligament. (Figure 3-9a) When no axial motion is allowed, the center of rotation is located at the level of the damper (which is acting as a type of “hinge”, Figure 3-9b). This shift in the center of rotation reduces the effective moment arm for L4 rotation, which in turn causes a reduced moment and lower stresses in the L3-L4 disc since L1 will have the same displacement in both cases. This allows a more physiological motion than can otherwise be obtained with instrumentation that does not allow distraction. As noted in the results, decreasing the R-parameter alone has the effect of reducing the stiffness of the material resisting the rotation, while decreasing the G-parameter alone has the effect of adjusting the axis of rotation for L4. The numerical results obtained in the present study demonstrate that within the range of values for stiffness and axial motion (parameters R and G) used herein, moving the center of rotation anteriorly is more effective in reducing stress amplitudes in the adjacent level disc than is reducing the elastic stiffness of the instrumentation. Although the particular type of dynamic instrumentation studied has both features, i.e., anterior translation of the center of rotation and reduced elastic stiffness, the former feature is considered to be clinically more important.

Increased load demands at the adjacent level disc accompanying fusion has been associated with accelerated degeneration of that disc in animal

models[14] and is also associated with adjacent level disc problems in humans[5]. Rigid fixation has been associated with increased pressures within the disc which are as much as 73% greater in adjacent cervical discs[84]. Others suggest that not just the amplitude, but the altered pattern of loading may also have a role in this process of adjacent level disc disease[12]. Given the current findings, some[6] argue that there remains less than adequate proof of the difference between rigid and dynamic stabilization, while others[10] claim that the lack of differences provides support for the concept. This assumption will be best evaluated from long-term follow-up data obtained from adequately powered randomized controlled clinical trials which study dynamic versus conventional instrumentation. It is important to remember that “dynamic” is an appellation for a generic class of load-sharing fixation instrumentation; due to differences in designs and materials of such devices, varying levels of stiffness and motion will result. Outcomes of computational or in vivo studies employing dynamic devices are likely to be different due to their biomechanical heterogeneity. Only the resulting clinical studies will enable those with superior performance to be identified.

Limitations of the present study include the less than ideal anatomical model used. The lumbar vertebrae employed in this finite element model were not size-adjusted for the various vertebral levels, but were all identical and based upon the dimensions of an L4 vertebral body. However, this model was developed and validated previously[74] and thus is not considered a major

limitation because the focus of the study was the comparative, not absolute, differences in pressures within the disc. Also, as loading deforms the in vivo spine, the load likely does not remain perpendicular: however for the model used in this study, it was assumed to remain perpendicular. This assumption introduces a limitation to the absolute accuracy of the internal stress results reported, but the magnitude of this error is considered small and the comparative (between rigid and dynamic stabilization instrumentation) effects are believed negligible. The model used also did not include the effects of degenerative disc material properties, strain dependent disc swelling pressures/material permeability, or nonlinear elastic material behavior. While these may be important from an absolute perspective to understand the behavior of individual discs[85], their relative contribution in the present study involving comparison of two different fixation types is considered insignificant.

Assuming that adjacent level disc deterioration is partially caused by repetitive high amplitude loading and non-physiologic axes of rotation, reduced elastic bending stiffness and increased axial motion attributable to an anteriorly shifted axis of rotation in posterior instrumentation will more favorably distribute the motion demands of the lumbar spine. This finding supports emerging clinical evidence that such mechanical alterations to posterior spinal fixation devices have a beneficial effect on disc tissue and thereby delays the onset, reduces the severity of, or prevents entirely, the phenomenon of accelerated adjacent level disc deterioration.

In conclusion, reducing the stiffness, increasing the axial motion, and anteriorly translating the axis of rotation of posterior spinal fixation instrumentation may be part of the solution to the problem of adjacent level disc degeneration.

CHAPTER 4 – BIOMECHANICAL TESTING OF FACET FUSION TECHNIQUE

4.1 - Introduction

Traditionally a pedicle screw system has been used for fixation of the lumbar spine and this involves major surgery and recovery time. Facet fixation is a technique that has been used for stabilization of the lumbar spine and the proposed facet fixation technique can be performed as a percutaneous procedure. The proposed technique stabilizes the facet joints in a similar manner as the translaminar facet stabilization.

Minimal invasive surgery has had an increase in popularity the last couple of years, instead of a traditionally open back surgery. For minimal invasive surgery, a facet fixation will be more feasible than a pedicle screw system[86]. The minimal invasive pedicle screw method is very time consuming and technically demanding.

The procedure discussed in this paper is a percutaneous facet fixation where an allograft is used for fixation. This method will use human bone for the fixation and this will allow the facets to fuse together and provide fixation of the facet joints. The stability of the functional spinal unit (FSU) will be restricted by no motion of the facet joint, which will lead to fusion of the facet joint. While all

other available procedures for FSU stabilization use pedicle or transfacet screw fixation, this procedure uses an allograft bone dowel that is pre-formed to a specific shape[22,87,88].

4.2 - Materials and Methods

Three human cadaveric lumbar spine segments were tested, using a nondestructive testing method. The lumbar spines were disarticulated at L1-L2 and L3-L4. The segments were tested in axial rotation, combined flexion/extension and lateral bending. The specimens were first tested intact as control. Next, the same spine segments were implanted with the facet fusion allograft by a board certified orthopedic surgeon according to the manufacturer's specification. Axial rotation, flexion/extension and lateral bending were performed with a constant load of 100 N and a moment of 6 Nm was applied in 6 cycles. The first 5 cycles were used to precondition the specimen and the data for the 6th cycle was interpreted.

4.2.1 - Spine Preparations

A total of three adult human cadaver lumbar spine segments were harvested. The donor's average age was 65.5 ± 1.8 (range 61-73) years and the donor group consisted of 2 males and 1 female. The medical history of all the donors was reviewed, where donors with any disease that will affect the

spine biomechanics or trauma were excluded. These three lumbar spine segments were investigated visually, as well as the specimens went through a radio graphically screening to exclude any major abnormalities such as osteolycis, fractures or damage to the vertebral bodies or the intervertebral disc. The disarticulation was chosen based on the quality of the particular articulations found in the radio graphically screening. The lumbar spines were disarticulated to create a variation of Functional Spinal Units (FSU) from different levels to be used in this study. This method allows for the most FSU's to be extracted from each lumbar spine, but certain spines produced more FSU's than others.

En Block specimens were stored at -80 degree Celsius and thawed to +4 degrees Celsius in a refrigerator. The specimens where covered by gauss, sprayed with saline solution and left at room temperature before testing. To securely attach the specimens to the test fixture, the specimens were reinforced by inserting metal screws in the vertebral endplate and potted in a two part polyepoxide based resin. All extraneous musculature was removed from each spine, keeping all the ligaments and posterior elements intact.

4.2.2 - Implant and Fixation Techniques

4.2.2.1 - Specimen Instrumentation

Each FSU was instrumented with facet fusion allograft as shown in Figures 4-1 and 4-2.

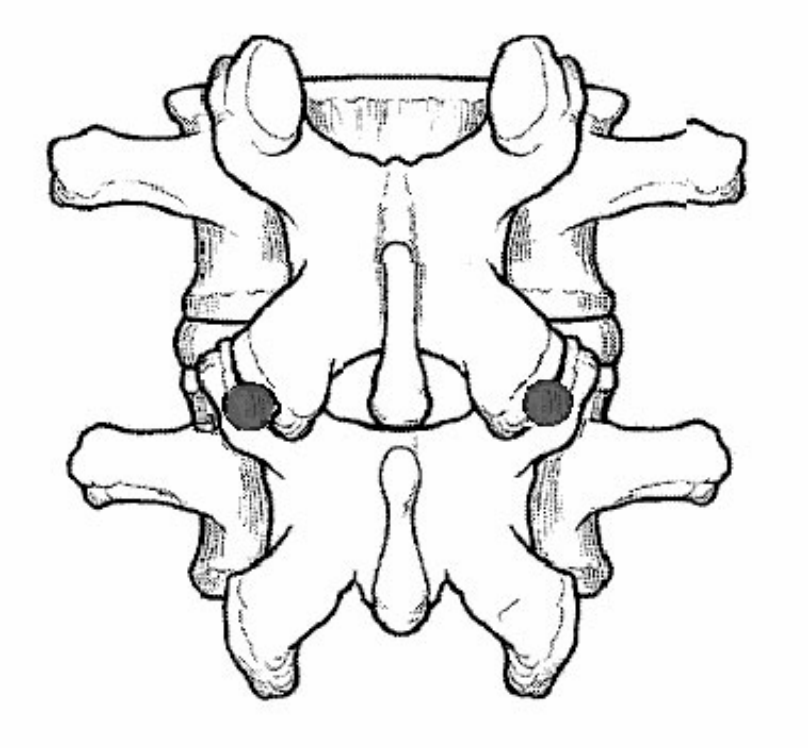

Figure 4-1: Posterior View of Placement of Facet Fusion Allograft in Facet Joints

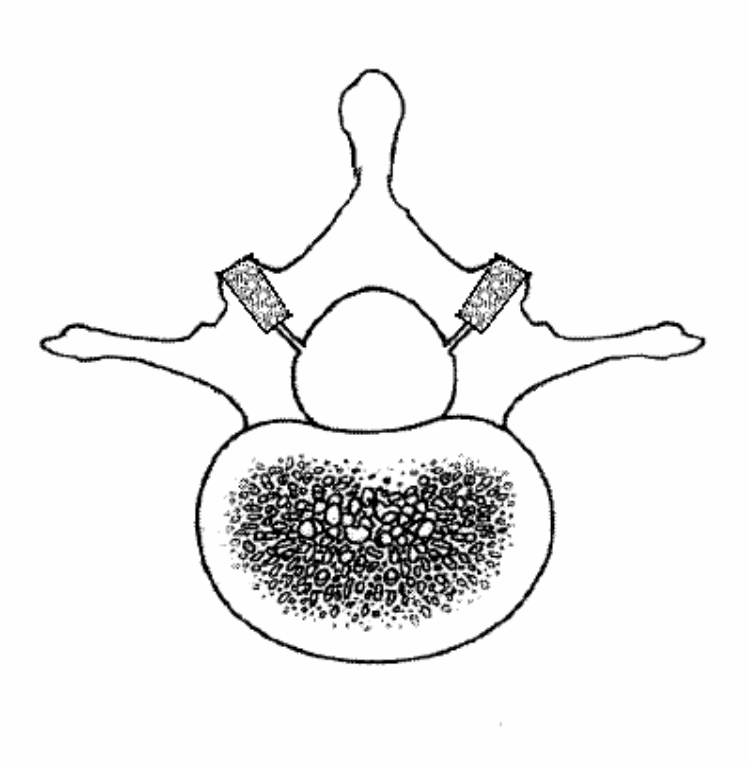

Figure 4-2: Superior View of Placement of Facet Fusion Allograft in Facet Joints.

4.2.2.2 - Facet Fusion Allograft Insertion

To implant the facet fusion allograft the facet joint needs to be accessed either by direct visualization during open surgery or indirectly by fluoroscopy during percutaneous surgery. Once the facet joint is identified, the posterior facet joint capsule is removed, as well as any significant osteophytes. The facet joints will then be cleared of any remaining cartilage or debris, as well as this, clinically, will help the joint to fuse. The drill guide is then centered between the inferior and superior facets, where the drill guide stabilizing teeth are placed

superior and inferior in the facet joint opening. This will prevent the drill guide to move around on the facets, but still allow for changing the angle medially and laterally to drill in the plane of the facet joint. Once the drill guide is in position, the tapered compaction drill bit can be used to drill facet implantation site. This will lead to a removal of less than 50% of the superior facet and less than 50% of the inferior facet as shown in Figure 4-3.

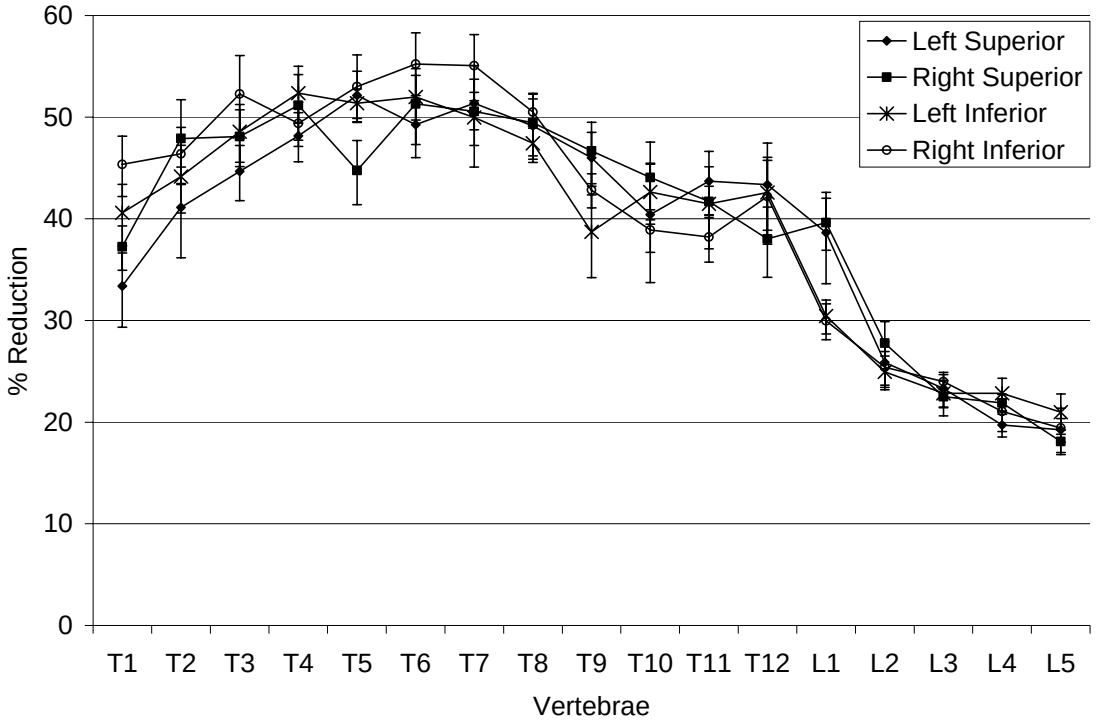

Figure 4-3: Percentage Reduction of Facet Joint Due to the Implant (Panjabi)

The drill bit has a drill stop set at 10 mm and it will allow the drill bit to drill slightly deeper (2 mm) than the height of the implant (8 mm), but not so deep it might cause any potential damage. The drill bit and drill guide is now

removed, and this void will now be filled with the tapered facet fusion allograft. The facet fusion allograft implant is inserted with the placement and impaction tool, in the same direction as the site was drilled. This implant is now impacted into place and will be counter sunk 1-2 mm into the compaction-drilled tunnel. This procedure will be repeated for the other facet joint at the particular level that is being treated.

4.2.3 - Study Protocol

The segments were tested in axial rotation, combined flexion/extension and combined left/right lateral bending. The specimens are tested intact (control) before they where treated with the facet fusion allograft implant. Axial rotation, flexion/extension and lateral bending were performed with a constant axial load of 100 N and a moment of 6 Nm was applied in 6 cycles. The loading rate used for all the different cases is 0.125 Hz for one part of the cycle[89].

4.2.4 - Statistical Analysis

The collected data was evaluated by using one-way analysis of variance (ANOVA) followed by a Tukey-Kramer comparison for evaluating the significant difference of the stiffness between the intact and treated specimen. All statistical tests were performed on SAS (release 9.1, SAS Institute Inc., Cary,

NC), with a significance defined at a 95% confidence interval. The values are given as the mean ± standard deviation.

4.3 - Results

The stiffness and range of motion (ROM) of intact and treated specimens, during flexion/extension, lateral bending and axial rotation are shown in Figures 4-1 and 4-2. Tables 4-1, 4-2 and 4-3 summarize the results of stiffness, ROM and percentage change due to treatment.

Table 4-1: Range of Motion of the Intact and Treated Segment

	Intact [Degree]	Treated [Degree]
Flexion	4.28 ± 1.10	1.59 ± 0.52
Extension	2.18 ± 0.58	1.03 ± 0.04
Bending	6.05 ± 0.56	3.12 ± 1.39
Torsion	2.51 ± 1.41	1.82 ± 0.64

Table 4-2: Stiffness of the Intact and Treated Segment

	Intact [Nm/Degree]	Treated [Nm/Degree]
Flexion	0.99 ± 0.25	2.45 ± 0.78
Extension	2.00 ± 0.74	4.11 ± 0.22
Bending	1.51 ± 0.16	3.56 ± 1.80
Torsion	3.64 ± 1.76	4.21 ± 1.29

Table 4-3: Percentage Change of Range of Motion and Stiffness

	Change of ROM	Change of Stiffness
Flexion	49.62% ± 10.73%	126.76% ± 35.71%
Extension	40.85% ± 21.02%	119.88% ± 4.16%
Bending	54.44% ± 13.84%	148.58% ± 48.78%
Torsion	26.32% ± 2.09%	26.80% ± 11.43%

In comparison to the intact specimen, the facet fusion allograft shows a significantly higher ($P < 0.05$) stiffness in flexion and extension (Table 4-1). There is a noticeable change of stiffness in lateral bending and axial rotation, but this change is not statistical significant. The stiffness increased 127% in

flexion (1.1 Nm/Degree to 2.5 Nm/Degree) and 120% in extension (1.8 Nm/Degree to 4.0 Nm/Degree) following bilateral implantation of the allograft. For lateral bending, the stiffness increased by 149% (1.6 Nm/Degree to 4.0 Nm/Degree) and for axial torsion there was a 27% change of stiffness (3.0 Nm/Degree to 3.8 Nm/Degree).

These values are interpreted from full range of motion grafts. The sample graph in figure 4-4 below, show the typical flexion-extension results.

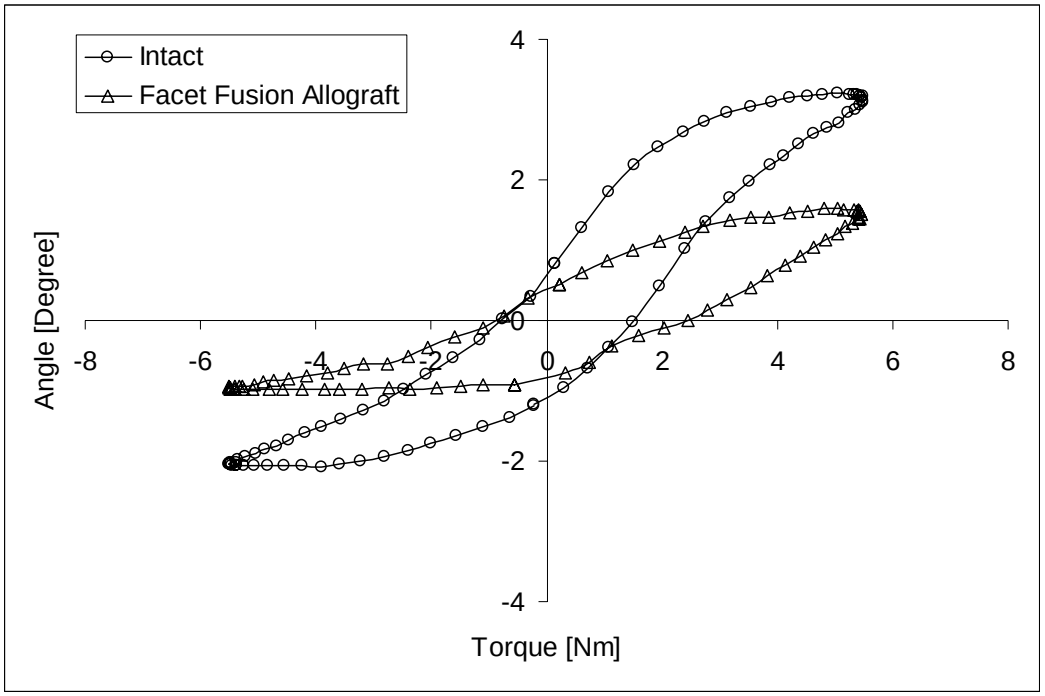

Figure 4-4: Typical Flexion-Extension Results, Showing Comparison Between Intact and Treated Specimen.

The sample graphs for lateral bending and axial rotation are shown in Appendix B.

4.4 - Discussion

Fixation of the facet joint has been performed by inserting metal screws perpendicular through the facet joint. This has shown to give a good fixation, but it is at high risk of causing permanent damage. It is also a technically demanding procedure[28-29,35-46]. The proposed technique is similar to the Lumbar Facet Interference screw, but this implant is made from allograft and has a press fit[27,86],. A potential problem with allograft implant is the biological process of absorption of the bone. When the bone is absorbed, the implant reduces in size and there is a chance of the implant to become loose[90-93]. This method is also very similar to the procedure proposed by Stein et al., while the proposed procedure has a pre shaped implant and the proper instruments for insertion[86]. The purpose of this study was to find the biomechanical stability of the facet fusion allograft and compare to published data of various facet fixation techniques[27].

There are some limitations in this study to consider. As any *in vitro* experimental testing, the study will be limited by the lack of muscular lumbar spine stability. This will be the case for all the groups included in this study, and the change as a percentage will be compared. Since each FSU is used for control and treatment, each FSU are tested twice. This might change the stiffness of the last treatment from fatigue, but according to Panjabi there is little or no effect for the short duration the specimen is tested[94].

Lumbar facet fixation devices have been discussed in several biomechanical *in vitro* studies[27]. These fixation methods provide good fixation, but they are technical demanding and the biomechanical properties are usually not ideal in axial rotation. This proposed method inserts the implant in the plane of the facet, perpendicular to the traditional method. For this reason, the implant is compressed between the inferior and superior facet and better axial rotation results are seen. The comparative intact and treated results for stiffness and range of motion are shown in figure 4-5 and 4-6 below.

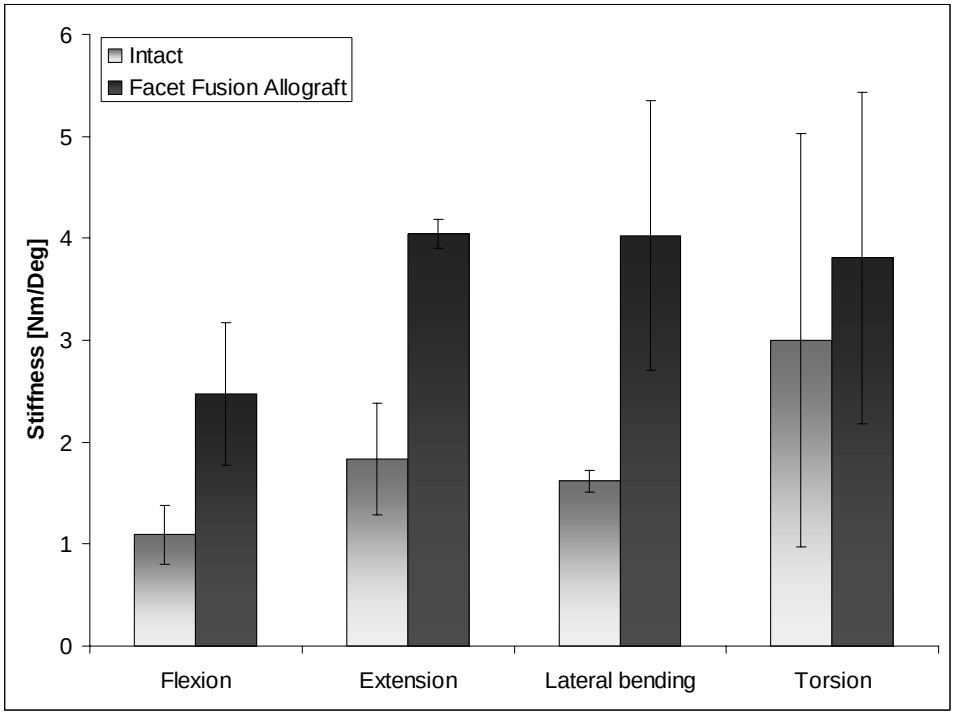

Figure 4-5: Stiffness Results for the Intact and Treated Specimens

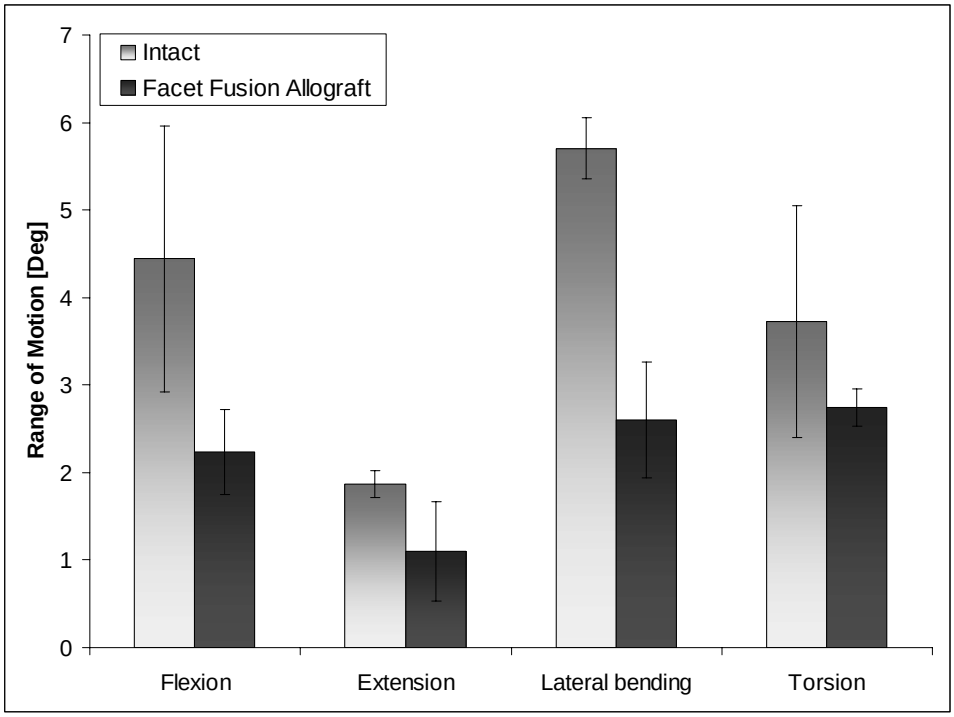

Figure 4-6: Stiffness Results for the Intact and Treated Specimens

The comparisons in difference between specimens are shown in Appendix B.

In the comparison shown in Figure 4-7, the facet fusion allograft is shown as a standalone procedure, while the other methods are presented with a cage. This might cause the facet fusion allograft to show a higher gain of stiffness in axial rotation.

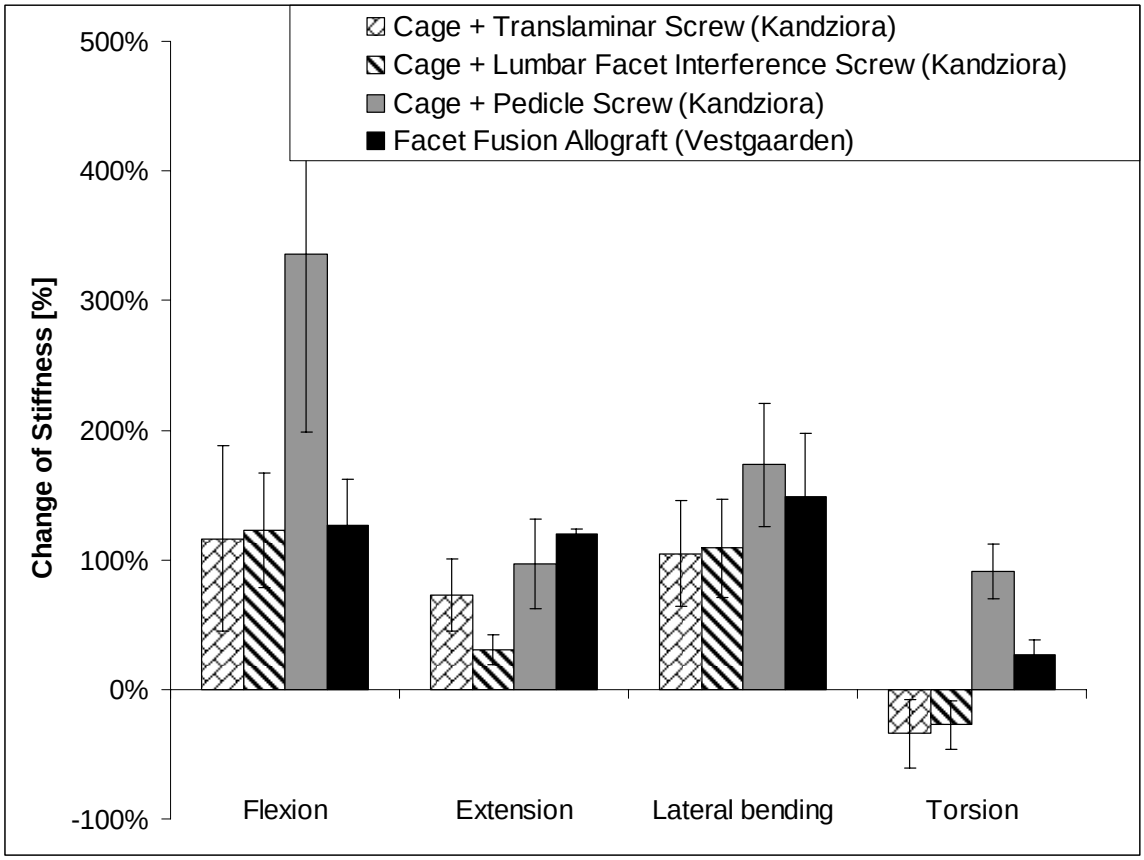

Figure 4-7: Comparison of Percent Change of Stiffness to Published Data

The facet fusion allograft presented in this study demonstrates comparable demobilization of flexion and extension to traditional methods. The percentage change of stiffness in lateral bending demonstrate a great percentage change, but it is not statistical significant. One out of three specimens only had a minor change in stiffness and therefore, the statistical significance is not present.

The stiffness of this fixation method is lower than the pedicle screw systems. This can be explained by the absence of metal through the pedicles,

which allows for deflection of the pedicle. Deflection of the pedicle also allows for some deflection of the vertebral body and higher stress level in the disc are occurring. By increased stress, the disc will remain in better condition and reduce the chance of adjacent degenerative disc desease[90-93].

The pre-shaped allograft dowel is effective in restricting facet joint movement. This method provides stabilization and fixation for minor instabilities, which can allow the joint to fuse through integration with the allograft. The allograft also gives a smooth change of stiffness in the spine and reduces the chance of adjacent degenerative disc disease. This study demonstrates that the biomechanical properties of the facet fusion allograft are similar to existing facet fixation methods. Results of this pilot study shows a potential for this technique and additional biomechanical studies with a greater sample size is desiered.

CHAPTER 5 - A COMPARISON BETWEEN *IN VIVO* AND *IN VITRO* INTRADISCAL PRESSURES

5.1 - Introduction

There is no data that explains the actual forces acting on the spine during flexion, extension, lateral bending or axial rotation. There are published articles that give intradiscal pressure measurements for these motions, but there are no correlation performed against *In Vitro* testing results. All these issues will be addressed in this dissertation and it will be presented in sections.

Many models have been made to estimate loads during lifting activity. Some are simplified, while others have used EMG measurements to find the muscle forces with or without the combination of intradiscal pressure measurements[95-109]. Wilke *et al* made continuous dynamic *In Vivo* measurements for flexion, extension, lateral bending and axial rotation[110]. This is the only published study with this data. The motions and pressure curves described in this study are very similar to experimental cadaver testing.

Finite Element Method has been used to evaluate spinal implants, but these models do not necessarily give a direct correlation to physiological loads acting on the spine[111-114]. By using known forces and moments, their respective

displacements and the use of intradiscal pressure, these models can be very accurate. There are models that take these aspects into considerations, but they are not validated by the use of physiological data[115-118].

The prediction of muscle forces and spinal loadings are dependent on the trunk models and the posture[119-120]. The effect of the abdominal pressure is controversially, but the *In Vivo* intradiscal pressure is measured with all the physiological loads present[121]. The abdominal pressures are usually not simulated during *In Vitro* testing or in analytical models.

There have been several papers published in the 60s and 70s discussing intradiscal pressures[122-127]. These pressures are absolute values, rather than complete data sets published more recently. Pressure transducers are also an important aspect of measuring intradiscal pressures and there has been made some major advantages with the technology used in more recent publications[66].

The purpose of this paper is to provide a database with correlation to previously published *In Vivo* intradiscal pressure curves to the current *In Vitro* pressure curves. This data will enable a proper adjustment and validation of a computer model and to give physiological meaning to loading data used on cadavers for *In Vitro* testing of medical devices.

5.2 - Materials and Methods

A study of the intradiscal pressure during motion of an intact specimen will be performed to compare to *In Vivo* results as described in literature.

Human cadaver lumbar spines were disarticulated to get functional spinal units (FSU). The FSU's were tested in combined axial compression and flexion/extension, combined axial compression and lateral bending and combined axial compression and axial rotation using a nondestructive testing method.

5.2.1 - Spine Preparations

A total of 6 adult human cadaver lumbar spine segments were harvested. The donor's average age was 50.5 ± 1.8 (range 45-65) years and the donor group consisted of 5 males and 1 female. The medical history of all the donors was reviewed, where donors with any disease that will affect the spine biomechanics or trauma were excluded. These six lumbar spines were investigated visually, as well as the specimens went through a radio graphically screening to exclude any major abnormalities such as osteolycis, fractures or damage to the vertebral bodies or the intervertebral disc. All the FSU's were disarticulated to give L4-L5 specimens containing the L4 and L5 vertebral bodies, posterior elements, ligaments and the intervertebral disc.

En Block specimens were stored at -20 degree Celsius and thawed to +4 degrees Celsius in a refrigerator[128]. The specimens where covered by gauss, sprayed with saline solution and left at room temperature prior to testing. To securely attach the specimens to the test fixture, the specimens were reinforced

by inserting metal screws in the vertebral endplate and potted in a two part polyepoxide based resin. All extraneous musculature was removed from each spine, keeping all the ligaments and posterior elements intact. Plain film radiographs (Faxatron Model Ni: MX-20, Wheeling, IL) was used to verify that none of the reinforcing metal screws interfered with the intervertebral disc.

5.2.2 - Test Setup and Biomechanical Testing

5.2.2.1 - Test Setup

A nondestructive spine biomechanics test setup was used to find the biomechanical properties. This particular setup is based on an axial servo-hydraulic materials testing system (MTS Systems Inc., 858 Bionix II, Eden Prairie, MN) and is modified to allow bending as well as axial rotation. Axial compression is integrated in the MTS 858 Bionix II and the load is measured by the use of a load cell. The load cell has an accuracy of 0.13% error for force measurements and 0.10% for displacement measurements. The linear variable differential transformers used to measure torsion have an approximate error of 1%.

The axial force and axial displacement are continuously recorded and can be used to interpret the axial stiffness of the specimen. Axial torsion is measured by fixing one end of the specimen and applying an axial torque on the other end of the specimen. By measuring the torque and the axial rotational

angle, the rotational resistance can be calculated. The bending consists of a superior and inferior moment and an equal, but opposite bending moment is applies at both ends. This allows for pure bending moment and no shear is present. The bending moment and the angle are recorded throughout the cycle for an accurate measurement of the bending stiffness. This bending moment is used to measure flexion/extension and by turning the specimen 90 degrees, it will measure lateral bending.

5.2.3 - Study Protocol

The segments were tested in axial rotation, combined flexion/extension and combined left/right lateral bending under constant axial compression.

Axial rotation, flexion/extension and lateral bending were performed with a constant load that represents the load of a person standing relaxed. From published data, the initial intradiscal pressure was set to 0.5 MPa and resulted in a constant axial compressive load of 500-700 N depending on the specimen[63-65,110,129-130]. A moment of 6 Nm was applied in 6 cycles. The loading rate used for all the different cases is 0.125 Hz for one part of the cycle.

With the pressure probe secured in the center of nucleus, the FSU was tested in all the motions and measurements were made. No losses of spinal fluids were noted during the pressure testing, while some of the specimens appeared to have severely dehydrated nucleus.

5.3 - Results

There have been previous studies that have reported *In Vivo* intradiscal pressures for daily activities. One study has reported series of data points during flexion-extension, lateral bending and axial rotation. These motions have been repeated *In Vitro*.

For this study, the comparable *In Vivo* intradiscal pressures are relaxed standing 0.43 - 0.50 MPa, standing flexed forward 1.08 MPa, standing extended backwards 0.6 MPa, lateral bending 0.59 MPa (decreasing to 0.38 MPa) and axial rotation 0.6 - 0.7 MPa[110].

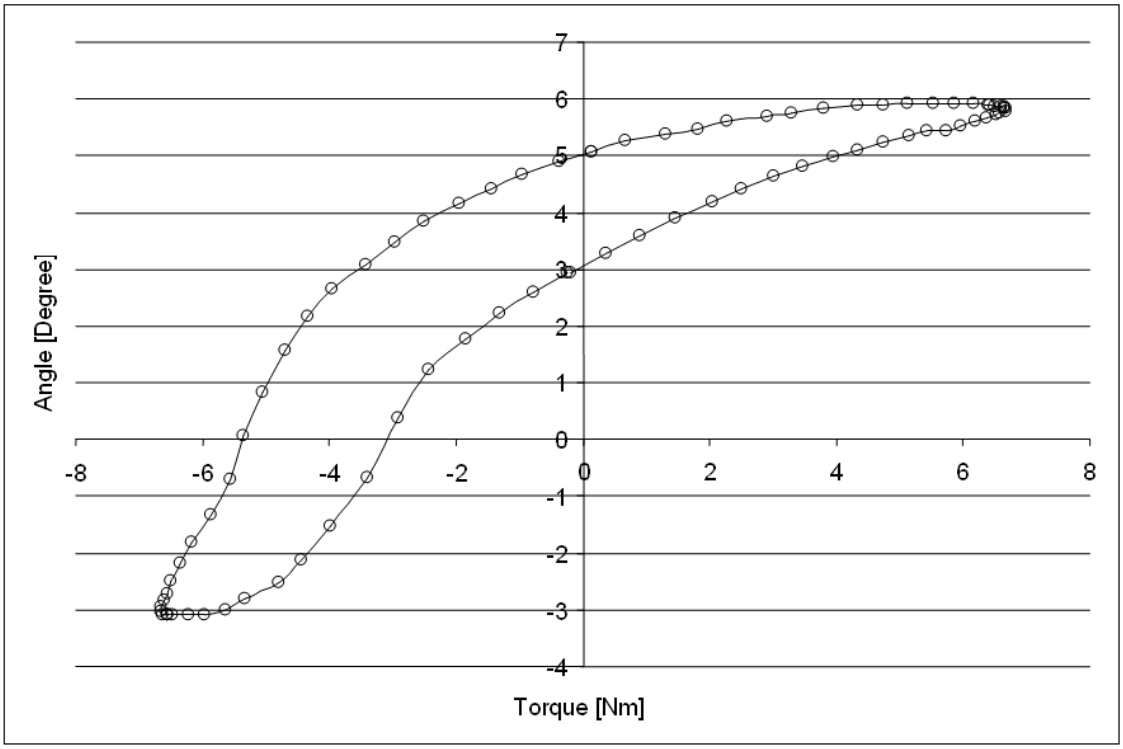

Figure 5-1: Torque vs. Angle Data for the Extension and Flexion Experimental Test

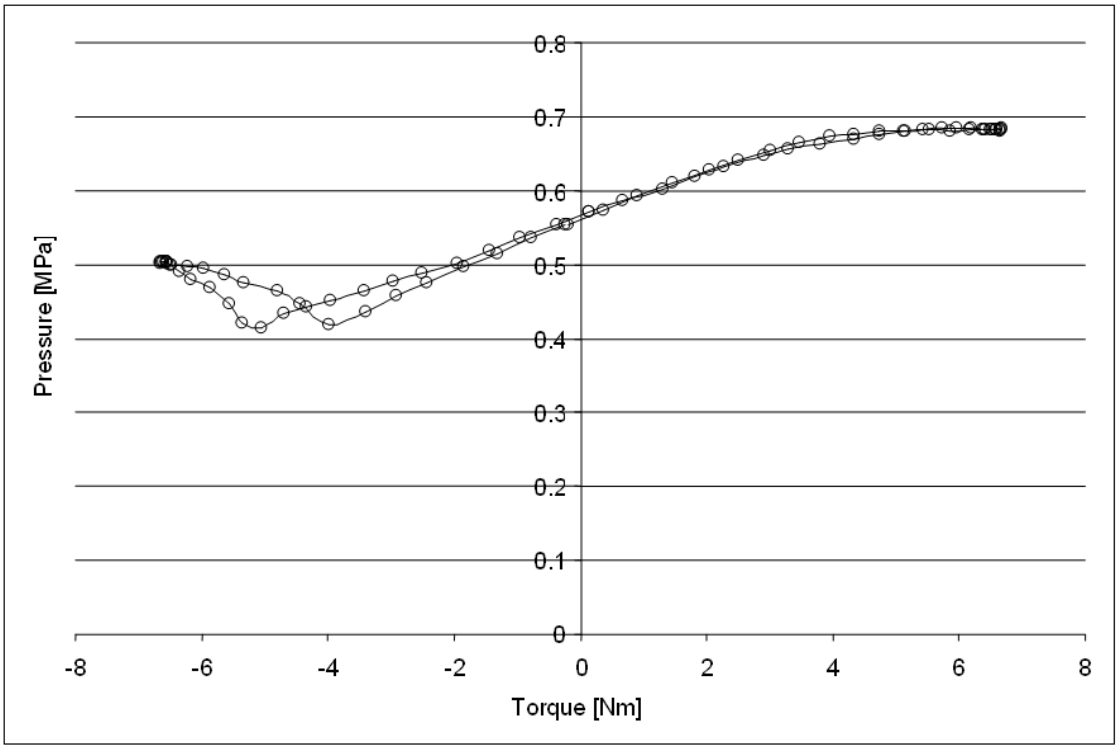

Figure 5-2: Pressure vs. Angle Data for the Extension and Flexion Experimental Test

In Vitro intradiscal results for the same motions are 0.68 MPa for flexion, 0.50 MPa in extension, 0.57 MPa during lateral bending (decreasing to 0.26 - 0.36 MPa) and axial rotation 0.51 - .53 MPa.

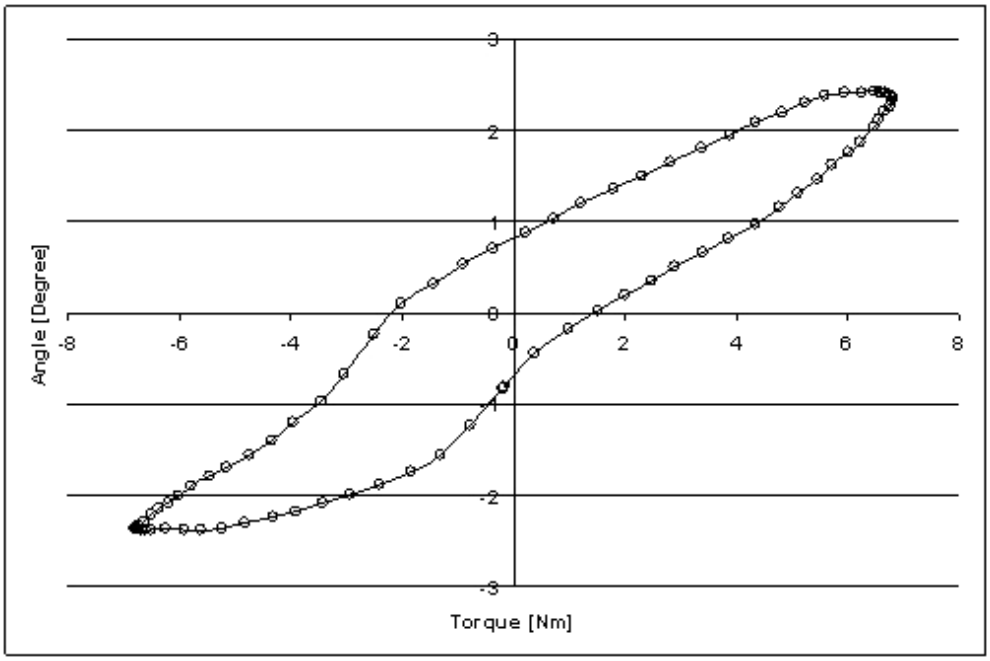

Figure 5-3: Torque vs. Angle Data for the Lateral Bending Experimental Test

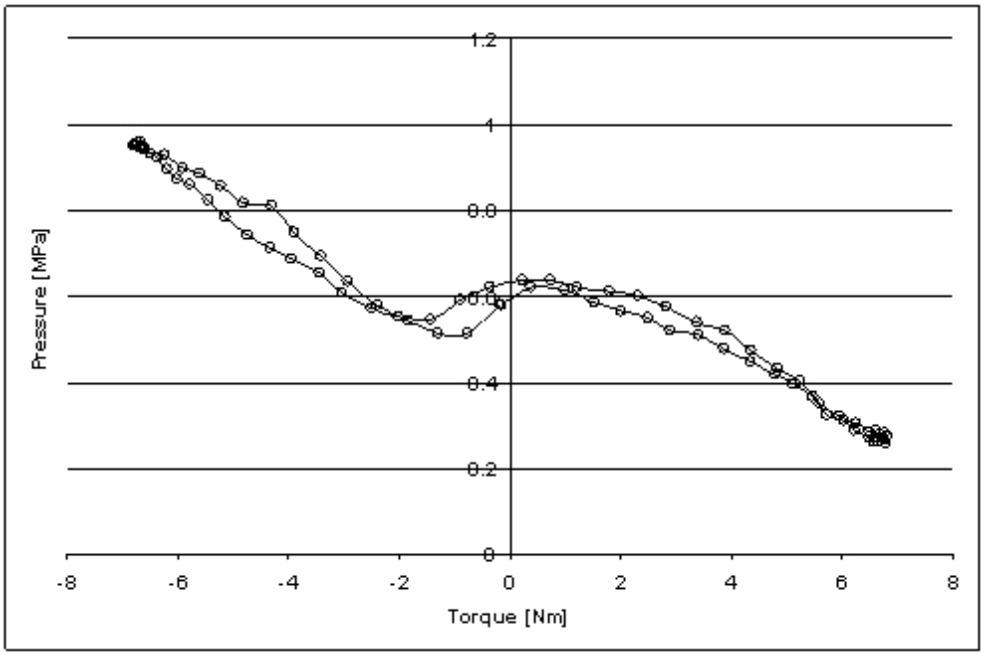

Figure 5-4: Pressure vs. Angle Data for the Lateral Bending Experimental Test

In Vitro results corresponds to the following moments and angular displacements; flexion 6.5 Nm and 5.9 degrees, extension 6.5 Nm and 3.1 degrees, lateral bending 1.8 Nm and 0.9 degree (decreased pressure at 6.3 Nm and 1.6 degrees) and axial rotation 3.6 - 5.7 Nm moment and 2.5 degrees angular displacement.

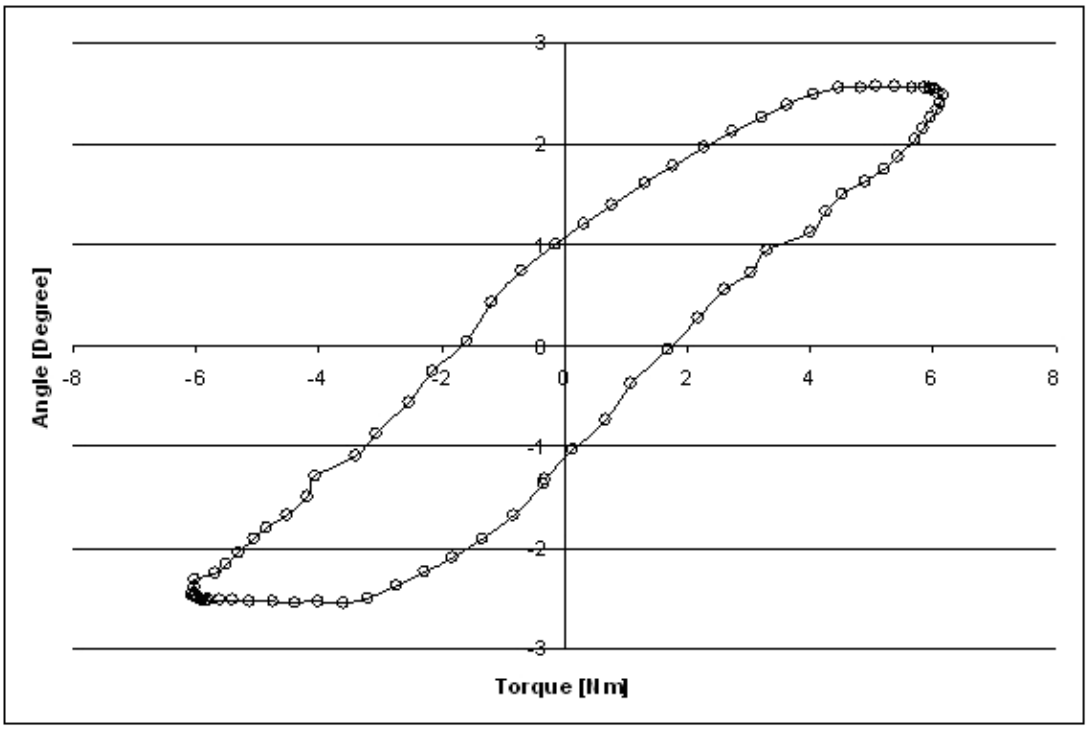

Figure 5-5: Torque vs. Angle Data for the Axial Rotation Experimental Test

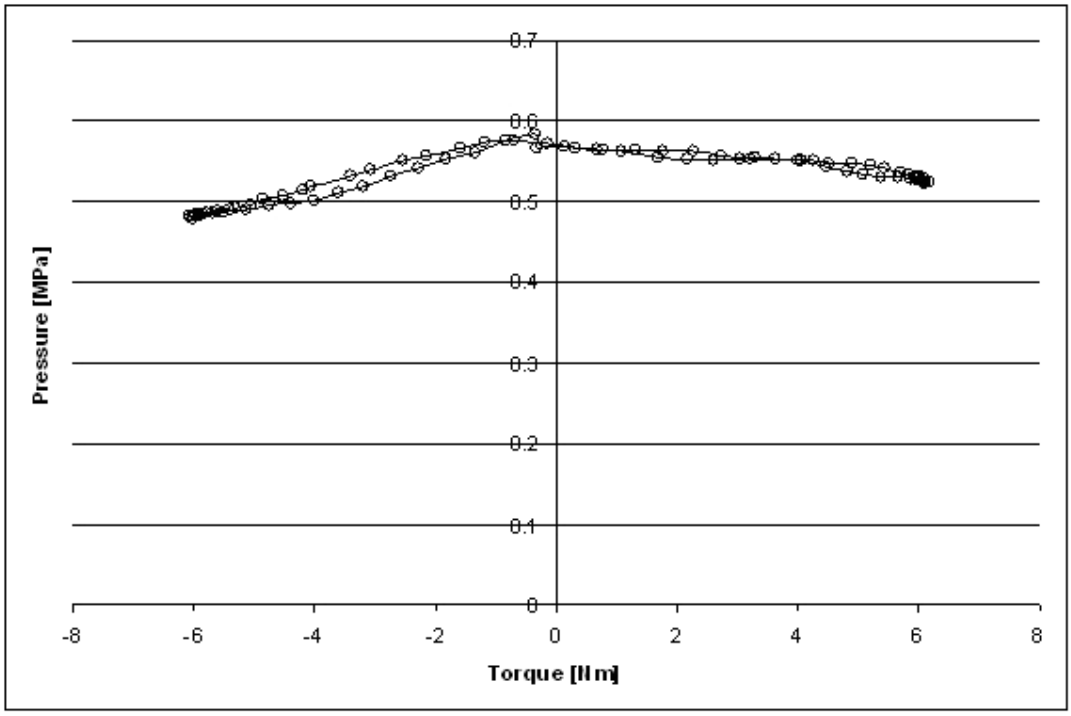

Figure 5-6: Pressure vs. Angle Data for the Axial Rotation Experimental Test

A comparison between the *In Vivo* and *In Vitro* curves are shown in Figures 5-7, 5-8 and 5-9.

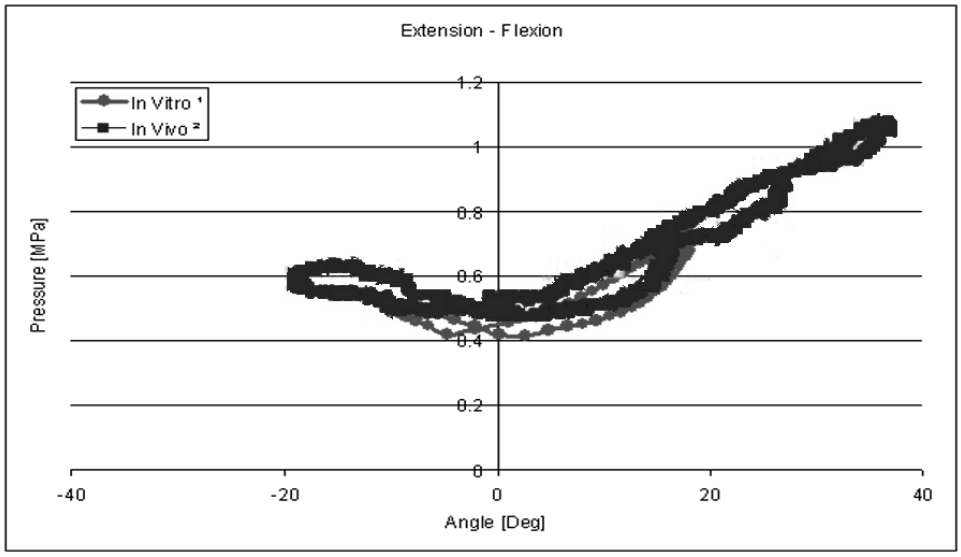

Figure 5-7: Extension - Flexion Intradiscal Pressure *In Vitro* of Selected L4-L5 Segments with Respect to the Total Motion in a Single Level

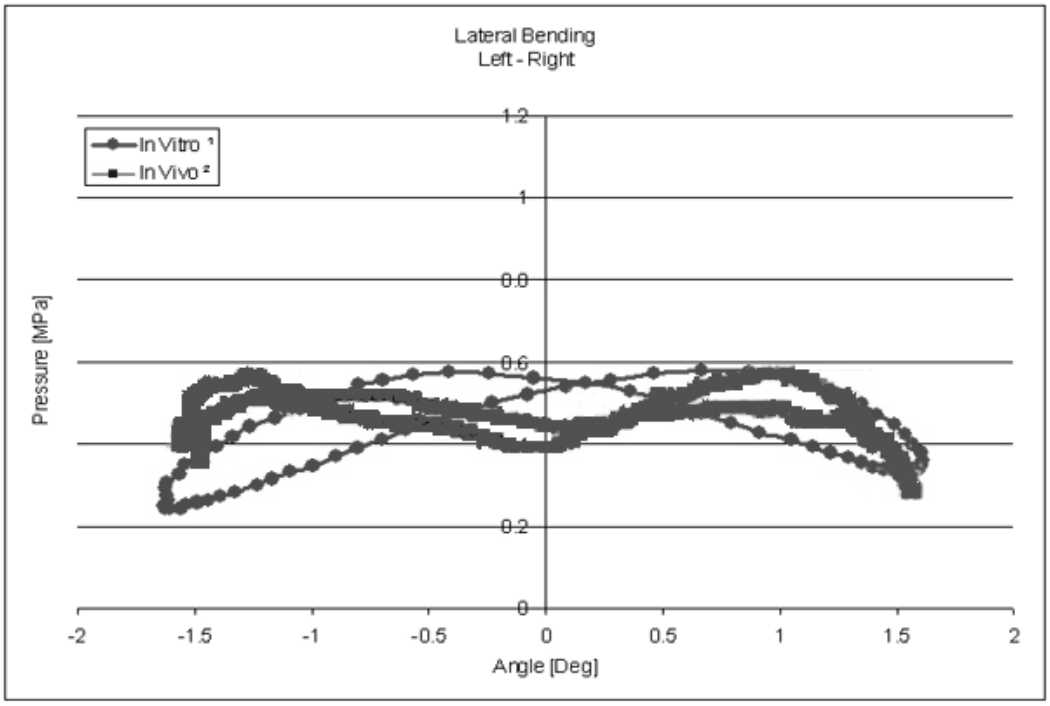

Figure 5-8: Lateral Bending Intradiscal Pressure *In Vitro* of Selected L4-L5 Segments with Respect to the Total Motion in a Single Level

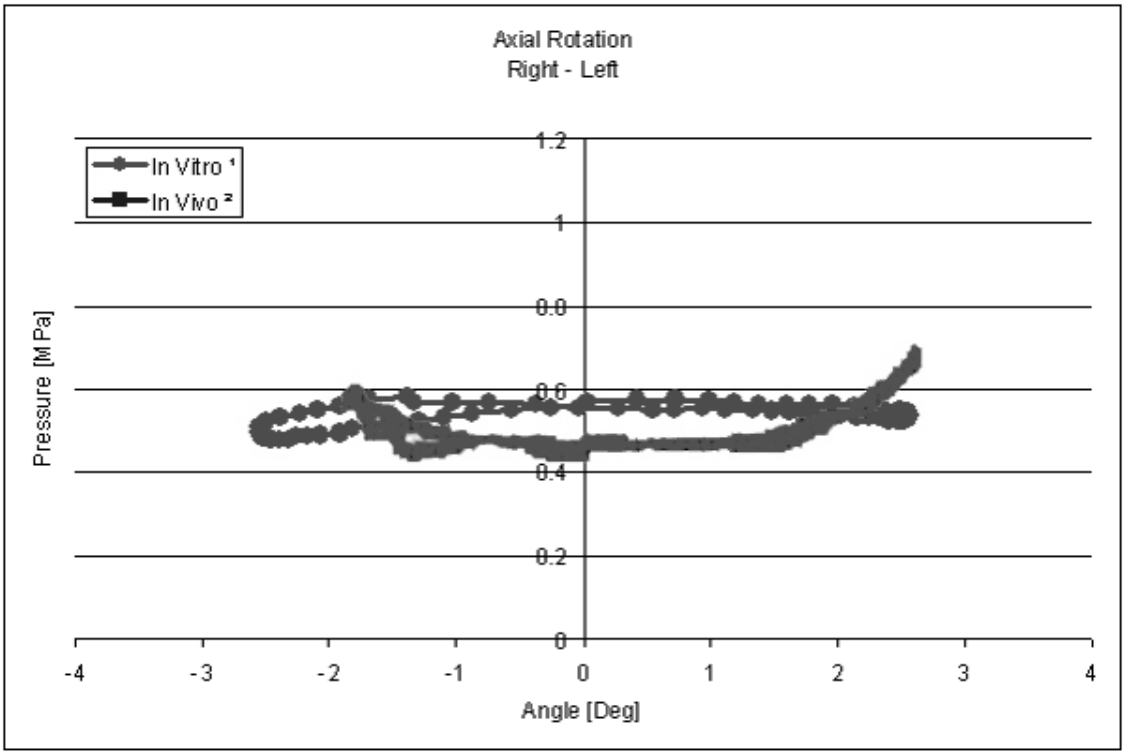

Figure 5-9: Axial Rotation Intradiscal Pressure *In Vitro* of Selected L4-L5 Segments with Respect to the Total Motion in a Single Level.

The line with square markers is an import from the *In Vivo* publication, while the measured *In Vitro* results are represented by circular marks.

5.4 - Discussion

The purpose of this study is to create a database of the correlation between *In Vivo* and *In Vitro* data. The *In Vivo* published pressure measurements have been used, where the *In Vitro* pressure measurements from the current study show a close relation to the *In Vivo* pressures[110]. This

database can be used for physiological relevance to experimental testing and for validation of mathematical models.

As far as the authors are aware, there has never been done a study to find these correlations. There are studies that show *In Vivo* intradiscal pressures, but the referred study is the only paper with dynamic *In* Vivo intradiscal pressure results published. During the testing of the cadaver spines, there were several specimens that could not reproduce the dynamic intradiscal pressures. These specimens were only used for the absolute values to achieve a reasonable sample size.

In present papers, the absolute values of the pressure in the center of L4-L5 are described as well. The values presented in this study are roughly the same to the values presented by Wilke *et al*, in exception of flexion and extension[110]. In flexion and extension, it is clear that the moments applied during the cadaver testing are not sufficient to achieve the pressures presented by Wilke *et. al.*[110] The flexion and extension results demonstrate a correlation, but the applied moments during *In Vitro* testing are not great enough to simulate the complete cycle of forward flexion and backwards extension. During *In Vitro* flexion and extension testing, the applied moment does not have to work against abdominal forces and pressures. This is not the case for *In Vivo*, and it is clear that this will create a higher moment to achieve the same pressure. This shows us that during biomechanical evaluation of medical devices, the applied

moment in flexion and extension needs to be greater than for lateral bending and axial rotation.

The results from the *In Vitro* testing give an accurate representation of the *In Vivo* intradiscal pressures during lateral bending. A symmetrical curve, roughly, is shown in lateral bending, with the same characteristics as seen during *In Vivo* measurements. It is seen both *In Vivo* and *In Vitro* that the pressure raises to a maximum, before the pressure decreases at the highest measured angular deflection. Wilke *et al* describes the possibility of muscles trying to stabilize the spine actively, before the muscles relaxed and stabilized the spine passively[110]. Since the same phenomenon is occurring *In Vitro*, this can be dismissed. A likely possibility is that the superior facet impacts the inferior facet on one side and acts like a pivot point. This will give increased disc height on one side of the disc and the chance of the nucleus to relieve pressure.

During axial rotation, the slope of the pressure is fairly stable for the *In Vitro* results. During *In Vivo* testing there is an increase of pressure at the end of the cycle. This can be explained by the axis of rotation being fixed during *In Vitro* testing and no translation allowed. This axis of rotation can have some translation *In Vivo*, were shear forces will be acting on the disc[131]. This could be the reason for the increased pressure observed by Wilke *et al*[110].

For all the specimens tested, the pressures at the maximum angular displacements were collected. These are similar to the pressures reported by Wilke *et al*, and these values are now verified by a higher sample size[110].

The published intradiscal pressure curves from the *In Vivo* measurements have a close correlation to the *In Vitro* measurements in the current study. This is a good guide for researchers to give a physiological relation to the loads that is applied during cadaver testing. It is very important to know how much load needs to be controlled by the implant. This can lead to optimization of implants and reduce the size.

During *In Vitro* flexion, the pure bending moment of 6.5 Nm gives an angular displacement of 5.9 degrees and an intradiscal pressure of 0.68 MPa. These measurements indicate that the physiological motion is equal to a flexion of 20 degrees. During *In Vitro* testing the physiological maximum flexion was not achieved, so higher moments should be applied during *In Vitro* testing. Similarly, during extension the angular displacement was 3.1 degrees and this gives an intradiscal pressure of 0.50 MPa and a physiological backwards extension of 10 degrees.

Lateral bending had pressure peak of 0.57 MPa when the angular displacement was 0.9 degree and at a bending moment of 1.8 Nm. This corresponds to a physiological lateral bending of 18 - 23 degrees. During lateral bending, the highest angular displacement of 1.6 degree was reached with a

moment of 6.3 Nm and a pressure of 0.26 - 0.36 MPa. This correlates to a person bending 29 degrees laterally.

An axial rotation of 2.5 degrees and a pressure of 0.51 - 0.53 MPa was achieved by applying a moment of 3.6 Nm to one side and 5.7 Nm to the other side. During *In Vivo* measurements, this same axial rotation gave 17 degree rotation to one side and 24 degrees to the other side.

Overall, this study found a good correlation between *In Vivo* and *In Vitro* data. The variation of data is likely to occur from lack of translation of motion during *In Vitro* testing. It is also shown that a higher moment needs to be applied during testing in Flexion/Extension. This can essentially be used to make physiological relation from experimental and analytical evaluations of the lumbar spine.

CHAPTER 6 – SUMMARY

6.1 – Conclusion

This dissertation contains both analytical and experimental hypothesis. Three hypotheses were looked at and all three hypotheses were answered. The first hypothesis was: The incidence of adjacent level disc disease in the lumbosacral spine will be decreased with the use of semi-rigid rods. As earlier shown in this dissertation, semi-rigid rods increase axial motion and anteriorly translating the axis of rotation. These factors reduce stress in adjacent disc, while maintains a stress level in the disc at the instrumented level. By reducing the stress in the adjacent disc, the disc will degrade at a lower rate, and the incident of adjacent level disc disease is decreased.

The second hypothesis was to validate increased biomechanical stiffness by the use of a facet fusion allograft *In Vitro*. It was found that facet fusion allograft significantly changes the stiffness and could be used for treatment of minor instability.

The last hypothesis to be answered was that there is a correlation between *In Vivo* and *In Vitro* intradiscal pressures. A comparison of the published *In Vivo* intradiscal pressures to *In Vitro* intradiscal pressures was

performed. The pressures were evaluated and the effects of loads applied *In Vitro* was considered. A clear correlation was found between the In Vivo and In Vitro intradiscal pressures and physiological relevance can be used In Vitro and in analytical models. This study also determined how much load to control while testing medical devices.

6.2 – Contribution

There are five important discoveries made in the research that has led to this dissertation. One of these is the discovery of reduced stresses in the adjacent disc by the use of semi-rigid rods. The incidence of adjacent level disc disease in the lumbosacral spine will be decreased with the use of semi-rigid rods. From this research, there has already been made improvements to this traditional fusion technique, and there are many patients that benefit from this. Semi-rigid rods also increase axial motion, anteriorly translating the axis of rotation, which leads to reduction of stress in adjacent disc.

Facet fusion has been performed since the 1940's, but it has always been a technically demanding procedure. Because of this, there has been very limited popularity to these methods. In this dissertation, a comparison of the biomechanical properties of a facet fusion allograft *In Vitro* was done. These results showed that there is merit for this procedure. Facet fusion allograft significantly changes the stiffness and could be used for treatment of minor instability.

Biomechanical testing of spinal implants has been performed on human cadaver lumbar spines, but there has never been any scientific reasoning for the loads that has been applied. There are several studies that look at the intradiscal pressures of living humans, and this data was used to find a correlation to the mechanical loads acting on the spine. These experimental results from the in vitro testing were compared to the published In Vivo intradiscal pressures. A clear correlation was found and physiological relevance can be used *In Vitro* and in analytical models, as well as a definition for how much load to control was found.

6.3 – Future Work

When conducting a intradiscal pressure study, it is important to have intervertebral discs that are in good shape and well hydrated. Also, with all biological tissue there will be differences. Therefore, a large study needs to be conducted to give the most optimal representation of the correlation between *In Vivo* and *In Vitro* intradiscal pressures. This study should also contain study parameters to give a good idea of the effect of different ligaments and facet joint capsule. Eventually, the intervertebral disc will be subjected to all independent loading situations, with all the ligaments and posterior elements removed. By removing all the ligaments and posterior elements, the disc can be modeled by using continuum mechanics. These specimens should also be tested at a series of different physiological strain rates.

All individual specimens used for this study, should also be scanned by high resolution Computed Tomography (CT) scans. These scans could be used to create a high quality three dimensional finite element mesh. This mesh can be created by using commercially available software, by importing the images into medical imaging software. In the selected software package, the tissue is selected a rendered into a three dimensional model. The rendering parameters are adjusted to accomplish the desired model. This model will be exported as a three dimensional model, before imported into a finite element mesher. Once the model is meshed, the exact experimental data for that particular finite element mesh can be created into a unique finite element model with verified values. This can be done to all of the individual specimens and statistical significance can be achieved by using finite element method.

With the current limited supply and increasing demand for human cadaver spines, there will be advantages of creating these verified and accurate finite element models. These models will reduce the demand for human cadaver spines. These models could also be used for preliminary testing of implants and have the design optimization performed at an early stage. These models can also be used to predict failures, instead of meeting the minimum requirements set by the Food and Drug Administration (FDA). The FDA, an American governmental agency, is already showing an interest in finite element modeling of medical devices.

REFERENCES

1. Wilke HJ, Neef P, Caimi M, et al. New in vivo measurements of pressures in the intervertebral disc in daily life. Spine 1999;24:755–62.

2. Schnake KJ, Schaeren S, Jeanneret B. Dynamic stabilization in addition to decompression for lumbar spinal stenosis with degenerative spondylolisthesis. Spine 2006;31:442-9.

3. Phillips FM, Voronov LI, Gaitanis IN, et al. Biomechanics of posterior dynamic stabilizing device (DIAM) after facetectomy and discectomy. Spine J 2006;6:714-22.

4. International Society of Biomechanics Homepage., 2004.

5. Gillet P. The fate of the adjacent motion segments after lumbar fusion. J Spinal Disord Tech 2003;16:338-45.

6. Korovessis P, Papazisis Z, Koureas G, et al. Rigid, semirigid versus dynamic instrumentation for degenerative lumbar spinal stenosis: a correlative radiological and clinical analysis of short-term results. Spine 2004;29:735-42.

7. Kumar MN, Jacquot F, Hall H. Long-term follow-up of functional outcomes and radiographic changes at adjacent levels following lumbar spine fusion for degenerative disc disease. Eur Spine J 2001;10:309-13.

8. Park P, Garton HJ, Gala VC, et al. Adjacent segment disease after lumbar or lumbosacral fusion: review of the literature. Spine 2004;29:1938-44.

9. Brechbuhler D, Markwalder TM, Braun M. Surgical results after soft system stabilization of the lumbar spine in degenerative disc disease--long-term results. Acta Neurochir (Wien) 1998;140:521-5.

10. Stoll TM, Dubois G, Schwarzenbach O. The dynamic neutralization system for the spine: a multi-center study of a novel non-fusion system. Eur Spine J 2002;11 Suppl 2:S170-8.

11. Wild A, Jaeger M, Bushe C, et al. Biomechanical analysis of Graf's dynamic spine stabilisation system ex vivo. Biomed Tech (Berl) 2001;46:290-4.

12. Mulholland RC, Sengupta DK. Rationale, principles and experimental evaluation of the concept of soft stabilization. Eur Spine J 2002;11 Suppl 2:S198-205.

13. Sengupta DK. Dynamic stabilization devices in the treatment of low back pain. Orthop Clin North Am 2004;35:43-56.

14. Mayer HM. The ALIF concept. EurSpineJ2000;9(suppl 1):S35– 43.

15. Regan JJ, Aronoff RJ, Ohnmeiss DD, et al. Laparoscopic approach to L4 –L5 for interbody fusion using BAK cages: experience in the .rst 58 cases. Spine1999;24:2171– 4.

16. Zdeblick TA, David SM. A prospective comparison of surgical approach for anterior L4 –L5 fusion: laparoscopic versus mini anterior lumbar interbody fusion. Spine2000;25:2682–7.

17. Zelle B, Konig F, Enderle A, et al. Circumferential fusion of the lumbar and lumbosacral spine using a carbon .ber ALIF cage implant versus autogenous bone graft: a comparative study. JSpinalDisordTech2002;15:369 –76.

18. Kanayama M, Cunningham BW, Haggerty CJ, et al. In vitro biomechanical investigation of the stability and stress-shielding effect of lumbar interbody fusion devices. JNeurosurg2000;93(suppl):259–65.

19. Tsantrizos A, Andreou A, Aebi M, et al. Biomechanical stability of .ve stand-alone anterior lumbar interbody fusion constructs. EurSpineJ2000; 9:14 –22.

20. Barnes B, Rodts GE, McLaughlin MR, et al. Threaded cortical bone dowels for lumbar interbody fusion: over 1-year mean follow-up in 28 patients. JNeurosurg2001;95(suppl):1– 4.

21. Lubbers T, Bentlage C, Sandvoss G. Anterior lumbar interbody fusion as a treatment for chronic refractory lower back pain in disc degeneration and spondylolisthesis using carbon cages-stand alone. ZentralblNeurochir2002; 63:12–17.

22. Jang JS, Lee SH, Lim SR. Guide device for percutaneous placement of trans-laminar facet screws after anterior lumbar interbody fusion. Technical note. JNeurosurg2003;98(suppl):100 –3.

23. Thalgott JS, Chin AK, Ameriks JA, et al. Minimally invasive 360 degrees instrumented lumbar fusion. EurSpineJ2000;9(suppl 1):S51–6.

24. Christensen FB, Hansen ES, Eiskjaer SP, et al. Circumferential lumbar spinal fusion with Brantigan cage versus posterolateral fusion with titanium Cotrel-Dubousset instrumentation: a prospective, randomized clinical study of 146 patients. Spine2002;27:2674–83.

25. Schofferman J, Slosar P, Reynolds J, et al. A prospective randomized com-parison of 270 degrees fusions to 360 degrees fusions (circumferential fu-sions). Spine2001;26:207–12.

26. Suk KS, Jeon CH, Park MS, et al. Comparison between posterolateral fusion with pedicle screw .xation and anterior interbody fusion with pedicle screw .xation in adult spondylolytic spondylolisthesis. YonseiMedJ2001;42: 316 –23.

27. Kandziora F, Schleicher P, Scholz M, et al. Biomechanical testing of the lumbar facet interference screw. Spine 2005; 30; E34-E39

28. King D. Internal .xation of lumbosacral fusion. J Bone Joint Surg Am 1948; 30:560–5.

29. Magerl F. Stabilization of the lower thoracic and lumbar spine with external skeletal .xation. Clin Orthop 1984;189:125–41.

30. Heggeness MH, Esses SI. Translaminar facet joint screw .xation for lumbar and lumbosacral fusion. A clinical and biomechanical study. Spine1991;16: S266 –9.

31. Kornblatt MD, Casey MP, Jacobs RR. Internal .xation in lumbosacral spine fusion. A biomechanical and clinical study. ClinOrthop1986;203:141–50.

32. Vanden Berghe L, Mehdian H, Lee AJ, et al. Stability of the lumbar spine and method of instrumentation. ActaOrthopBelg1993;59:175– 80.

33. Ferrara LA, Secor JL, Jin BH, et al. A biomechanical comparison of facet screw .xation and pedicle screw .xation: effects of short-term and long-term repetitive cycling. Spine2003;28:1226 –34.

34. Deguchi M, Cheng BC, Sato K, et al. Biomechanical evaluation of translami-nar facet joint .xation. A comparative study of poly-L-lactide pins, screws, and pedicle .xation. Spine1998;23:1307–12.

35. Benini A, Magerl F. Selective decompression and translaminar articular facet screw .xation for lumbar canal stenosis and disc protrusion. Br J Neurosurg 1993;7:413–8.

36. Boucher HH. Method of spinal fusion. Clin Orthop 1997;335:4–9.

37. Graham CE. Lumbosacral fusion using internal .xation with a spinous pro-cess for the graft: a review of 50 patients with a .ve-year maximum follow-up. Clin Orthop 1979;140:72–7.

38. Grob D, Humke T. Translaminar screw .xation in the lumbar spine: tech-nique, indications, results. Eur Spine J 1998;7:178–86.

39. Grob D, Rubeli M, Scheier HJ, et al. Translaminar screw .xation of the lumbar spine. Int Orthop 1992;16:223–6.

40. Heggeness MH, Esses SI. Translaminar facet joint screw .xation for lumbar and lumbosacral fusion: a clinical and biomechanical study. Spine 1991;16(6 Suppl):S266–9.

41. Humke T, Grob D, Dvorak J, et al. Translaminar screw.xation of the lumbar and lumbosacral spine: a 5-year follow-up. Spine 1998;23:1180–4.

42. Jacobs RR, Montesano PX, Jackson RP. Enhancement of lumbar spine fu-sion by use of translaminar facet joint screws. Spine 1989;14:12–5.

43. Margulies JY, Seimon LP. Clinical ef.cacy of lumbar and lumbosacral fusion using the Boucher facet screw .xation technique. Bull Hosp Jt Dis 2000;59: 33–9.

44. Plotz GM, Benini A. Anterior lumbar vertebral translation following trans-laminar screw .xation: a report of .ve cases. Int Orthop 1998;22:77–81.

45. Reich SM, Ku.ik P, Neuwirth M. Translaminar facet screw .xation in lum-bar spine fusion. Spine 1993;18:444–9.

46. Stonecipher T, Wright S. Posterior lumbar interbody fusion with facet-screw .xation. Spine 1989;14:468–71.

47. Blumenthal S, Gill K. Complications of the Wiltse Pedicle Screw Fixation System. Spine 1993;18:1867–71.

48. Esses SI, Sachs BL, Dreyzin V. Complications associated with the technique of pedicle screw .xation: a selected survey of ABS members. Spine 1993;18: 2231–8, discussion 2238–9.

49. Georgis T, Rydevik B, Weinstein JN, et al. Complications of pedicle screw .xation. In: Gar.n SR, ed. Complications of Spine Surgery. Baltimore: Wil-liams & Wilkins; 1989:200–10.

50. Gertzbein SD, Robbins SE. Accuracy of pedicular screw placement in vivo. Spine 1990;15:11–4.

51. Ginsburg HH, Scoles PV. Scoliosis Research Society Morbidity and Mortal-ity Committee: Complication Report 1990. Park Ridge, IL: Scoliosis Re-search Society; 1990.

52. Hsu J, Zuckermann JF, White AH, et al. Internal.xation with pedicle screws. In: White AH, Rothman RH, Roy CD, eds. Lumbar Spine Surgery. St. Louis: Mosby; 1987:322–38.

53. Lonstein JE, Denis F, Perra JH, et al. Complications associated with pedicle screws. J Bone Joint Surg Am 1999;81:1519–28.

54. Okuyama K, Abe E, Suzuki T, et al. Posterior lumbar interbody fusion: a retrospective study of complications after facet joint excision and pedicle screw .xation in 148 cases. Act Orthop Scand 1999;70:329–34.

55. Steffe AD, Biscup RS, Sitkowski DJ. Segmental spine plate with pedicle screw .xation: a new internal .xation device for disorders of the lumbar and thoracolumbar spine. Clin Orthop 1986;203:45–54.

56. Weinstein JN, Spratt KF, Spengler D, et al. Spinal pedicle .xation: reliability and validity of roentgenogram-based assessment and surgical factors on successful screw placement. Spine 1988;13:1012.

57. Whitecloud TS, Butler JC, Cohen JL, et al. Complications with the variable spinal plating system. Spine 1989;14:472–6.

58. Yahiro MA. Comprehensive literature review: pedicle screw .xation devices. Spine 1994;19(20 Suppl):2274S–8S.

59. Niosi CA, Oxland TR. Degenerative mechanics of the lumbar spine. Spine J 2004;4(suppl 6):202– 8.

60. van Deursen DL, Snijders CJ, van Dieen JH, et al. The effect of passive vertebral rotation on pressure in the nucleus pulposus. J Biomech 2001;34: 405–8.

61. van Deursen DL, Snijders CJ, Kingma I, et al. In vitro torsion-induced stress distribution changes in porcine intervertebral discs. Spine 2001;26:2582–6.

62. Janevic J, Ashton-Miller JA, Schultz AB. Large compressive preloads decrease lumbar motion segment flexibility. J Orthop Res 1991;9:228–36.

63. Wang JL, et al. The dynamic response of L(2)/L(3) motion segment in cyclic axial compressive loading. Clin Biomech (Bristol, Avon) 1998;13(suppl 1): 16–25.

64. Wilke HJ, Claes L, Schmitt H, et al. A universal spine tester for in vitro experiments with muscle force simulation. Eur Spine J 1994;3:91–7.

65. Wilke HJ, Wolf S, Claes LE, et al. Influence of varying muscle forces on lumbar intradiscal pressure: an in vitro study. J Biomech 1996;29:549–55.

66. Cakir B, Ulmar B, Koepp H, et al. [Posterior dynamic stabilization as an alternative for dorso-ventral fusion in spinal stenosis with degenerative instability]. Z Orthop Ihre Grenzgeb 2003;141:418-24.

67. McNally DS, Adams MA, Goodship AE. Development and validation of a new transducer for intradiscal pressure measurement. J Biomed Eng 1992; 14:495–8.

68. Grob D, Benini A, Junge A, et al. Clinical experience with the Dynesys semirigid fixation system for the lumbar spine: surgical and patient-oriented outcome in 50 cases after an average of 2 years. Spine 2005;30:324-31.

69. McNally DS, Adams MA. Internal intervertebral disc mechanics as revealed by stress profilometry. Spine 1992;17:66–73.

70. Markwalder TM, Wenger M. Dynamic stabilization of lumbar motion segments by use of Graf's ligaments: results with an average follow-up of 7.4 years in 39 highly selected, consecutive patients. Acta Neurochir (Wien) 2003;145:209-14; discussion 14.

71. Yantzer BK, Freeman TB, Lee WE, et al. Torsion-induced pressure distribution changes in human intervertebral discs

72. Saxler G, Wedemeyer C, von Knoch M, et al. [Follow-up study after dynamic and static stabilisation of the lumbar spine]. Z Orthop Ihre Grenzgeb 2005;143:92-9.

73. Adams MA, Freeman BJ, Morrison HP, et al. Mechanical initiation of intervertebral disc degeneration. Spine 2000;25:1625-36.

74. Bose B. Anterior cervical arthrodesis using DOC dynamic stabilization implant for improvement in sagittal angulation and controlled settling. J Neurosurg Spine 2003;98:8-13.

75. Kanayama M, Hashimoto T, Shigenobu K, et al. Adjacent-segment morbidity after Graf ligamentoplasty compared with posterolateral lumbar fusion. J Neurosurg Spine 2001;95:5-10.

76. Putzier M, Schneider SV, Funk J, et al. [Application of a dynamic pedicle screw system (DYNESYS) for lumbar segmental degenerations - comparison of clinical and radiological results for different indications]. Z Orthop Ihre Grenzgeb 2004;142:166-73.

77. Smit TH, Odgaard A, Schneider E. Structure and function of vertebral trabecular bone. Spine 1997;22:2823-33.

78. Martinez JB, Oloyede VO, Broom ND. Biomechanics of load-bearing of the intervertebral disc: an experimental and finite element model. Med Eng Phys 1997;19:145-56.

79. Vena P, Franzoso G, Gastaldi D, et al. A finite element model of the L4-L5 spinal motion segment: biomechanical compatibility of an interspinous device. Comput Methods Biomech Biomed Engin 2005;8:7-16.

80. White AA, Panjabi M. Clinical Biomechanics of the Spine. Second ed. Philadephia: Lippincott, 1990.

81. Goel VK, Monroe BT, Gilbertson LG, et al. Interlaminar shear stresses and laminae separation in a disc. Finite element analysis of the L3-L4 motion segment subjected to axial compressive loads. Spine 1995;20:689-98.

82. Niosi CA, Zhu QA, Wilson DC, et al. Biomechanical characterization of the three-dimensional kinematic behaviour of the Dynesys dynamic stabilization system: an in vitro study. Eur Spine J 2006;15:913-22.

83. Schmoelz W, Huber JF, Nydegger T, et al. Dynamic stabilization of the lumbar spine and its effects on adjacent segments: an in vitro experiment. J Spinal Disord Tech 2003;16:418-23.

84. Xu HZ, Wang XY, Chi YL, et al. Biomechanical evaluation of a dynamic pedicle screw fixation device. Clin Biomech (Bristol, Avon) 2006;21:330-6.

85. Chen CS, Cheng CK, Liu CL, et al. Stress analysis of the disc adjacent to interbody fusion in lumbar spine. Med Eng Phys 2001;23:483-91.

86. Zander T, Rohlmann A, Burra NK, et al. Effect of a posterior dynamic implant adjacent to a rigid spinal fixator. Clin Biomech (Bristol, Avon) 2006;21:767-74.

87. Eck JC, Humphreys SC, Lim TH, et al. Biomechanical study on the effect of cervical spine fusion on adjacent-level intradiscal pressure and segmental motion. Spine 2002;27:2431-4.

88. Natarajan RN, Williams JR, Andersson GB. Recent advances in analytical modeling of lumbar disc degeneration. Spine 2004;29:2733-41.

89. Stein M, Elliott D, Glen J, Morava-Protzner I: Young Investigator Award: Percutaneous facet joint fusion—Preliminary experience. J Vasc Interv Radiol 4:69–74, 1993.

90. Foley KT, Gupta SK. Percutaneous pedicle screw .xation of the lumbar spine: preliminary clinical results. JNeurosurg2002;97(suppl):7–12.

91. Verheyden P, Katscher S, Schulz T, et al. Open MR imaging in spine surgery: experimental investigations and .rst clinical experiences. EurSpineJ 1999; 8:346 –53.

92. Wilke HJ, Wenger K, Claes L. Testing criteria for spinal implants: recom-mendations for the standardization of in vitro stability testing of spinal implants. EurSpineJ1998;7:148 –54.

93. Benzel EC.Biomechanics of Spine Stabilization. Rolling Meadows, IL: American Association of Neurological Surgeons; 2001.

94. Cheng BC, Moore DK, Zdeblick TA, et al. Load-Sharing Characteristics of Two Anterior Cervical Plate Systems. The Cervical Spine Research Society Meeting; Rancho Mirage, California; 1997.

95. Treharne RW. Review of Wolff's law and its proposed means of operation. Orthop Rev 1981;10:35.

96. Wolff J. Das Gesetz der Transformation der Knochen. Berlin: Hirschwald Verlag; 1892.

97. Panjabi, M. M., Krag, M., Summers, D. et al. Biomechanical time-tolerance of fresh cadaveric human spine specimens. J Orthop Res. 1985;3(3):292-300.

98. Bradford FK, Spurling RG. The intervertebral disc. In: Charles C. Thomas, Springfield, 1945.

99. Morris JM, Lucas DB, Bresler B. Role of the trunk in stability of the spine. J Bone Jt Surg [Am] 1961;42-A(3):327-51.

100. Dieen JJv, Creemers M, Draisma I, Toussaint HM. Repetitive lifting and spinal shrinkage, effects of age and lifting technique. Clin Biomech 1994;9:367-74.

101. Looze MPd, Kingma I, Thunissen W, Wijk van MJ, Toussaint HM. The evaluation of a practical model estimating lumbar moments in occupational activities. Ergonomics 1994;38:1993-2006.

102. Gagnon D, Gagnon M. The influence of dynamic factors on triaxial net muscular moments at the L5/S1 joint during asymmetrical lifting and lowering. J Biomech 1992;25(8):891-901.

103. Marras WS, Sommerich CM. A three-dimensional motion model of laods on the lumbar spine: I. Model structure. Hum Factors 1991;33:123-37.

104. Hughes RE, Bean JC, Chan DB. Evaluating the effect of co-contraction in optimization models. J Biomech 1995;28(7):875-8.

105. Jager M, Luttmann, A. The load on the lumbar spine during asymmetrical bi-manual materials handling. Ergonomics 1992;35(7-8):783-805.

106. Hughes RE, Chan DB. The effect of strict muscle stress limits on abdominal muscle force predictions for combined torsion and extension loadings. J Biomech 1995;28(5):527-33.

107. Plamondon A, Gagnon M, Gravel D. Moments at the L5/S1 joint during asymmetrical lifting: effects of different load trajectories and initial load positions. Clin Biomech 1995;10(3):128-36.

108. Cappozzo A. Compressive loads in the lumbar vertebral column during normal level walking. J Orthop Res 1984;1:292-301.

109. Khoo BC, Goh JC, Bose K. A biomechanical model to determine lumbosacral loads during single stance phase in normal gait. Med Eng Phys 1995;17(1):27-35.

110. Cromwell R, Schultz AB, Beck R, Warwick D. Loads on the lumbar trunk during level walking. J Orthop Res 1989;7(3):371-7.

111. Schultz A, Andersson G, Ortengren R, Haderspeck K, Nachemson A. Loads on the lumbar spine. Validation of a biomechanical analysis by measurements of intradiscal pressures and myoelectric signals. J Bone Joint Surg Am 1982;64:713-20.

112. Wilke HJ, Neef P, Barbara H, et al. Intradiscal pressure together with anthropometric data – a data set for the validation of models. Clinical Biomechanics 2001;16:S111-S126.

113. Chaffin D. A computerised biomechanical models - development and use in studying gross body actions. J Biomech 1969;2:429-41.

114. McGill SM, Norman RW. Dynamically and statically determined low back moments during lifting. J Biomech 1985;18(12):877-85.

115. McGill SM, Norman RW. Partitioning of the L4-L5 dynamic moment into disc, ligamentous and muscular components during lifting. Spine 1986;11(7):666-78.

116. McGill SM. Estimation of force and extensor moment contributions of the disc and ligaments at L4/L5. Spine 1988;13:1395-402.

117. Shirazi-Adl A. Finite-element evaluation of contact loads on facets of an L2-L3 lumbar segment in complex loads. Spine 1991;16(5):533-41.

118. Shirazi-Adl A. Nonlinear stress analysis of the whole lumbar spine in torsion- mechanics of facet articulation. J Biomech 1994;27(3):289-99.

119. Goel VK, Komg W, Han JS, Weinstein JN, Gilbertson L. A combined finite element and optimization investigation of lumbar spine mechanics with and without muscles. Spine 1993;18(11):1531-41.

120. Lavaste F, Skalli W, Robin S, Roy-Camille R, Mazel C. Three-dimensional Geometrical and Mechanical Modeling of the Lumbar Spine. J Biomech 1992;25(10):1153-64.

121. Parnianpour M, Wang JL, Shirazi-Adl A, Sparto P, Wilke H-J. The effect of variations in trunk models in predicting muscle strength and spinal loading. J musculoskeletal Res 1997;1:55-69.

122. Shirazi-Adl A, Parnianpour M. Role of posture in mechanics of the lumbar spine in compression. J Spinal Disord 1996;9(4):277-86.

123. Pope MH. Biomechanics of the lumbar spine. Ann Med 1989;21(5):347-51.

124. Nachemson A. The influence of spinal movements on the lumbar intradiscal pressure and on the tensile stresses in the annulus fibrosus. Acta Orthop Scand 1963;33:183-207.

125. Nachemson A, Elfstrom G. Intravital dynamic pressure measurements in lumbar discs. A study of common movements, maneuvers and exercises. Scand J Rehabil Med Suppl 1970;1:1-40.

126. Nachemson A. The effect of forward leaning on lumbar intradiscal pressure. Acta Orthop Scand 1965;35:314-28.

127. Nachemson A. In vivo discometry in lumbar discs with irregular necleograms. Acta Orthop Scand 1965;36:418-34.

128. Nachemson A. The load on lumbar disks in different positions of the body. Clin Orthop 1966;45:107-22.

129. Nachemson A, Morris JM. J Bone Jt Surg. In vivo Measurements of Intradiscal Pressure 1964;46-A(5):1077-92.

130. Dhillon N, Bass EC, Lotz JC. Effect of frozen storage on the creep behavior of human intervertebral discs. Spine 2001;26:883–8.

131. Mimura M, Panjabi MM, Oxland TR, et al. Disc degeneration affects the multidirectional flexibility of the lumbar spine. Spine 1994;19:1371–80.

132. McMillan DW, McNally DS, Garbutt G, et al. Stress distributions inside intervertebral discs: the validity of experimental 'stress profilometry.' Proc Inst Mech Eng H 1996;210:81–7.

133. White III AA, Panjabi MM. Spinal kinematics. The Research Status of Spinal Manipulative Therapy. NINCDS Monograph (No. 15), p. 93. Washington, D.C., U.S. Department of Health, Education and Welfare, 1975.

APPENDICES

Appendix A – Figures Related to Analytical Results

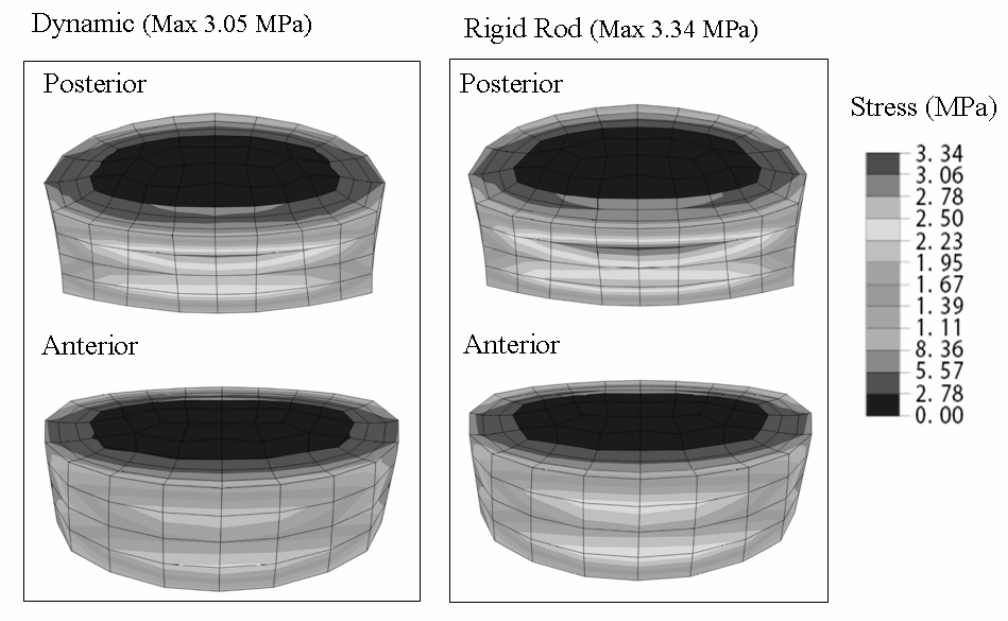

Figure A-1: Stress Distribution of L3-L4 Disk at 15˚ Flexion

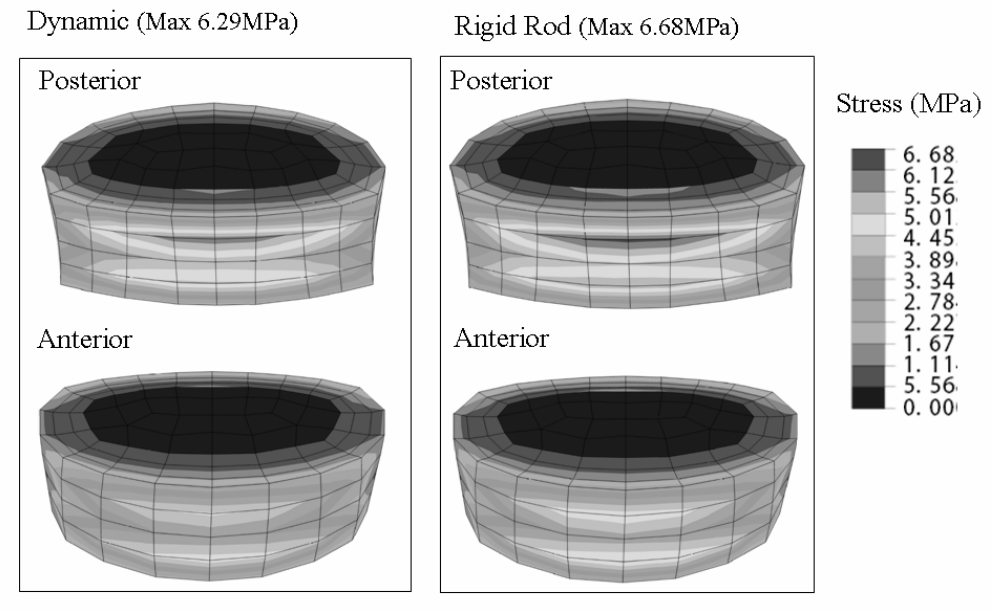

Figure A-2: Stress Distribution of L3-L4 Disk at 30˚ Flexion

Appendix A. (Continued)

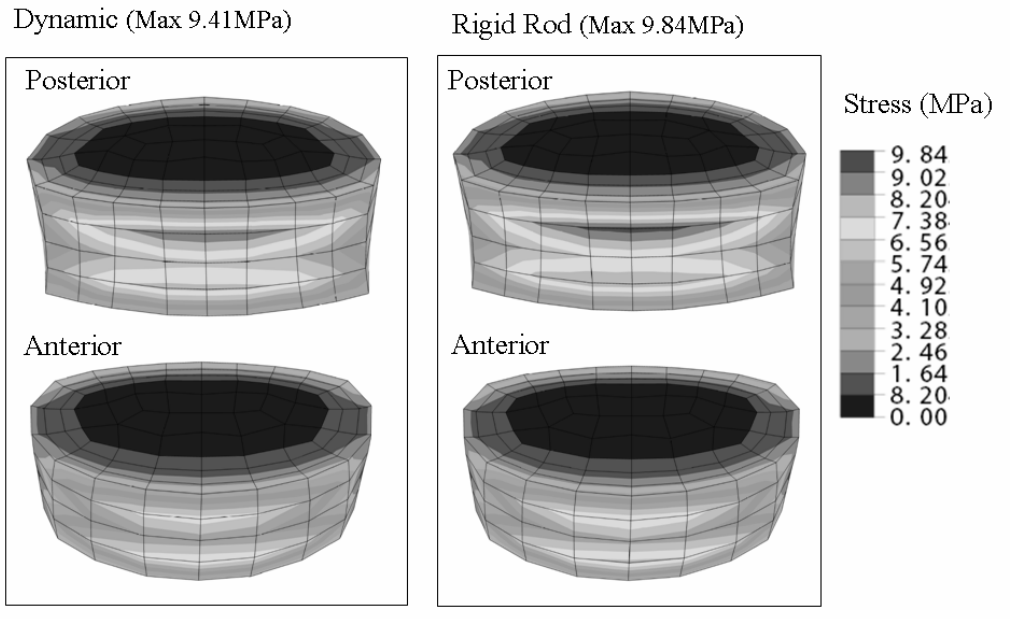

Figure A-3: Stress Distribution of L3-L4 Disk at 45˚ Flexion

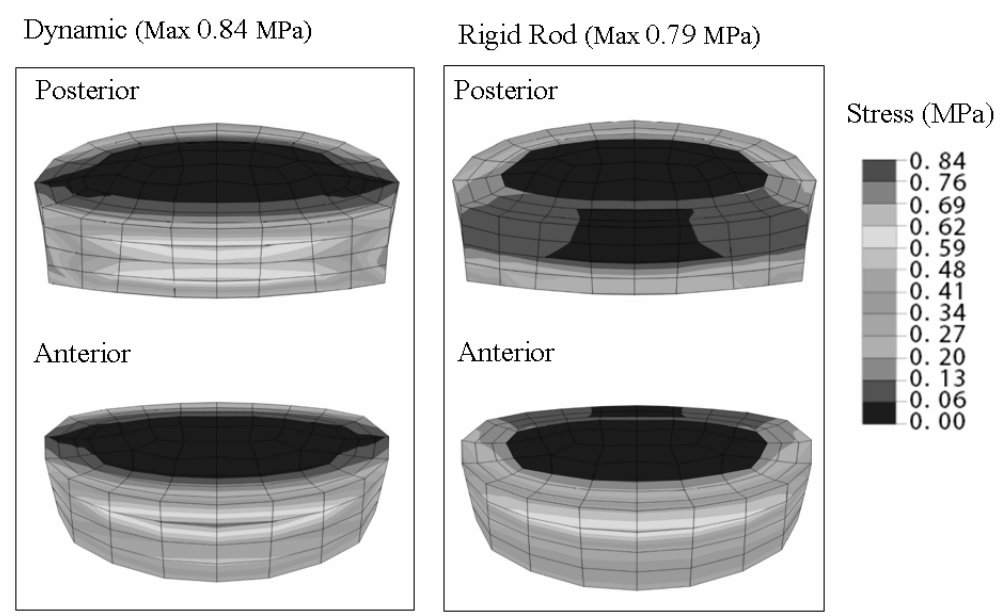

Figure A-4: Stress Distribution of L4-L5 Disk at 15˚ Flexion

Appendix A. (Continued)

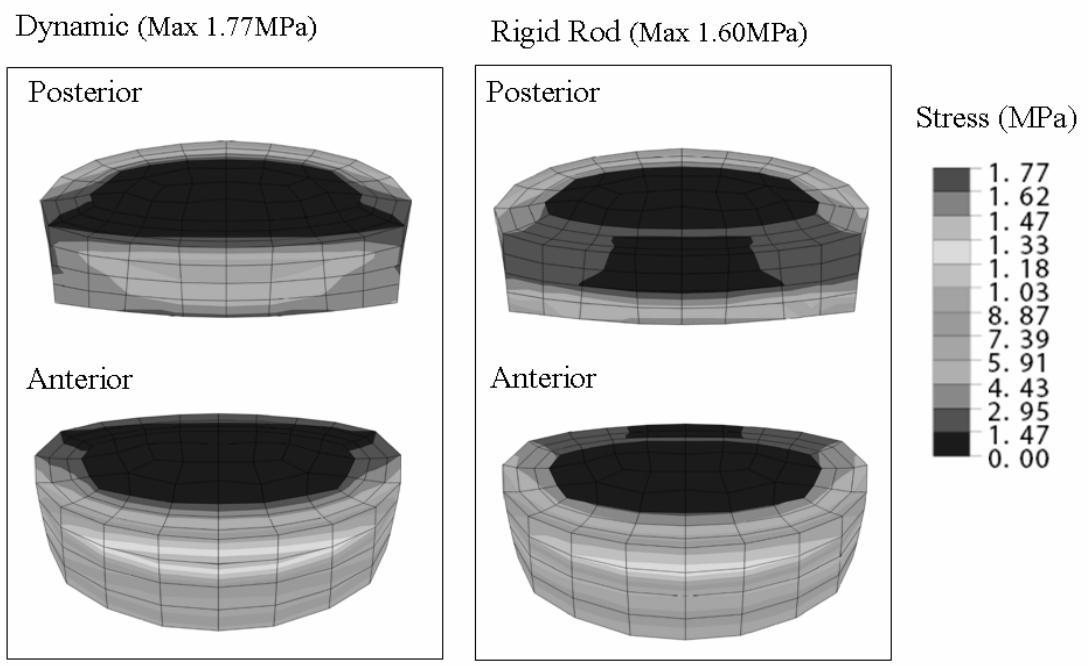

Figure A-5: Stress Distribution of L4-L5 Disk at 30˚ Flexion

Appendix B – Figures Related to Experimental Results

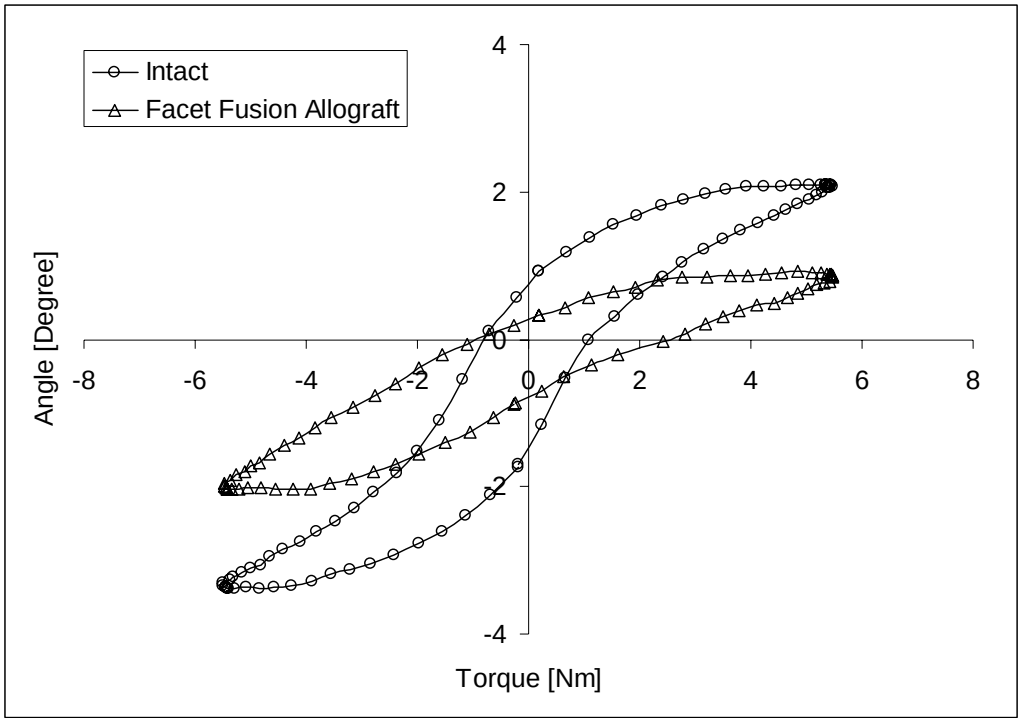

Figure B-1: Typical Lateral Bending Results, Demonstrating a Comparison Between Intact and Treated Specimen

Appendix B. (Continued)

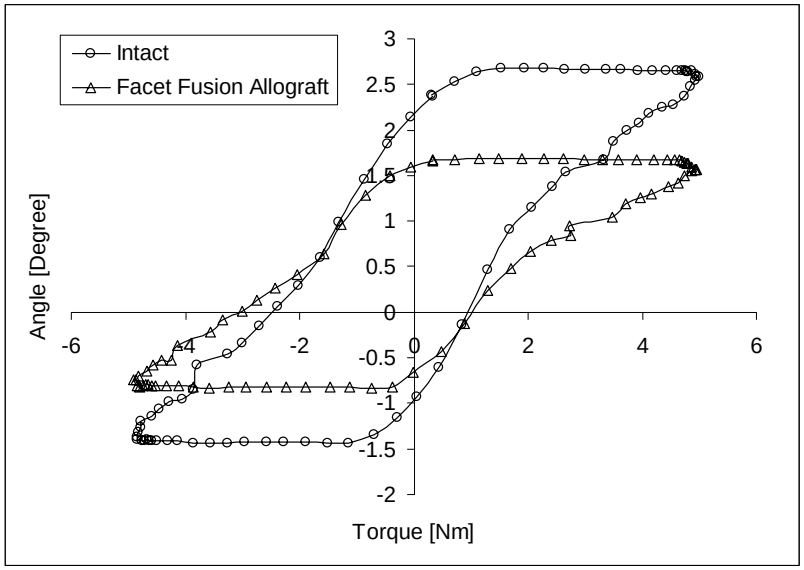

Figure B-2: Typical Axial Rotation Results, Demonstrating Comparison Between Intact and Treated Specimen

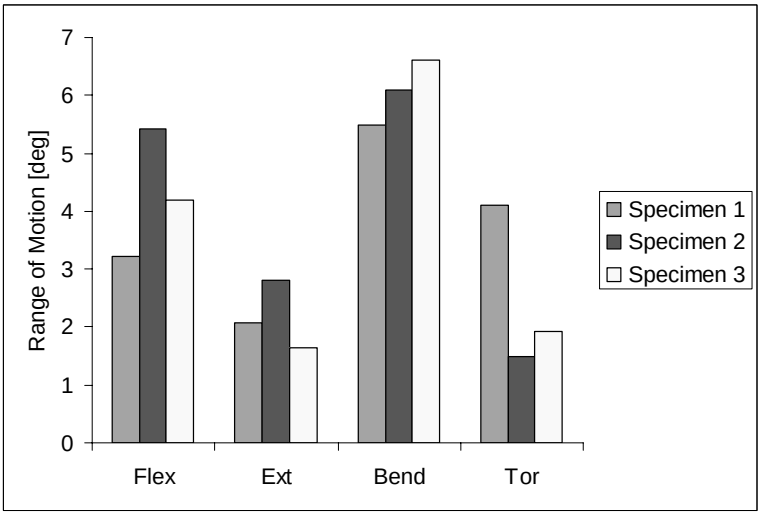

Figure B-3: Range of Motion Comparison Between the Different Intact Specimens

Appendix B. (Continued)

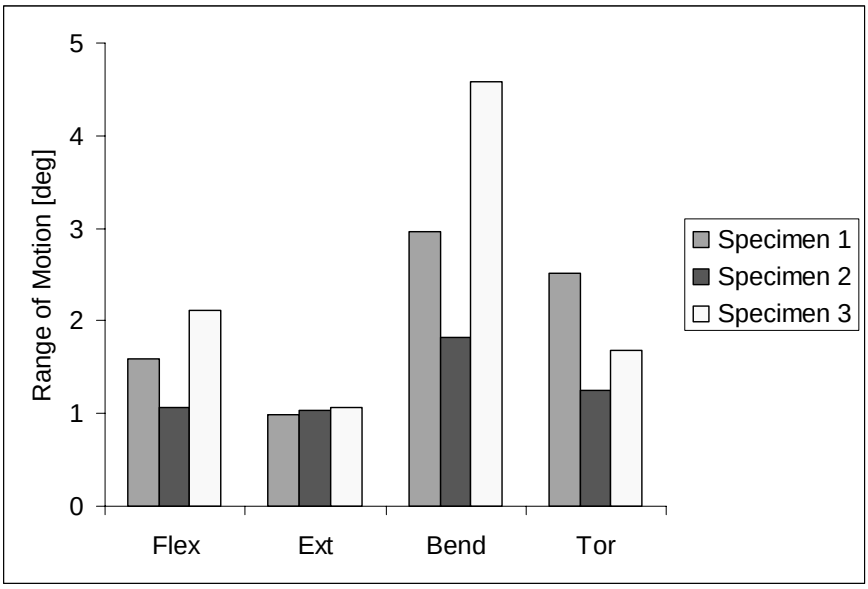

Figure B-4: Range of Motion Comparison Between the Different Treated Specimens

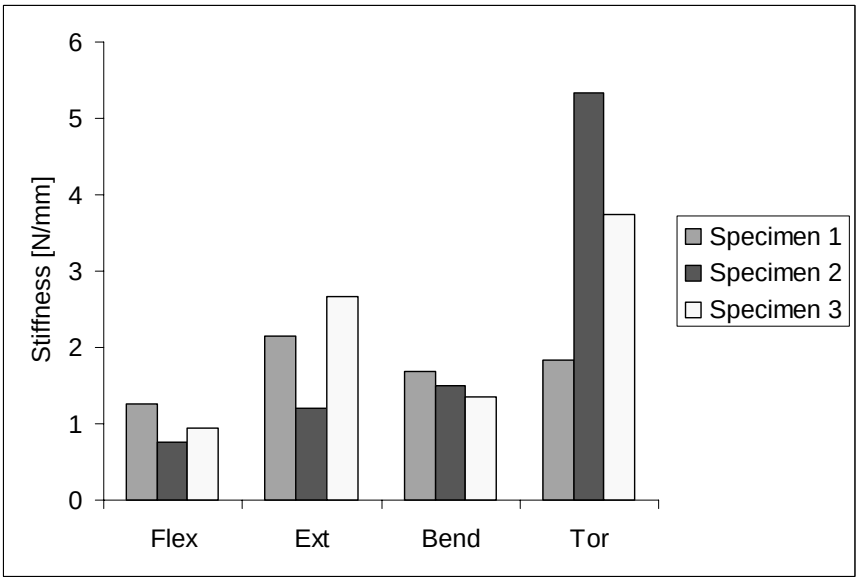

Figure B-5: Stiffness Comparison Between the Different Intact Specimens

Appendix B. (Continued)

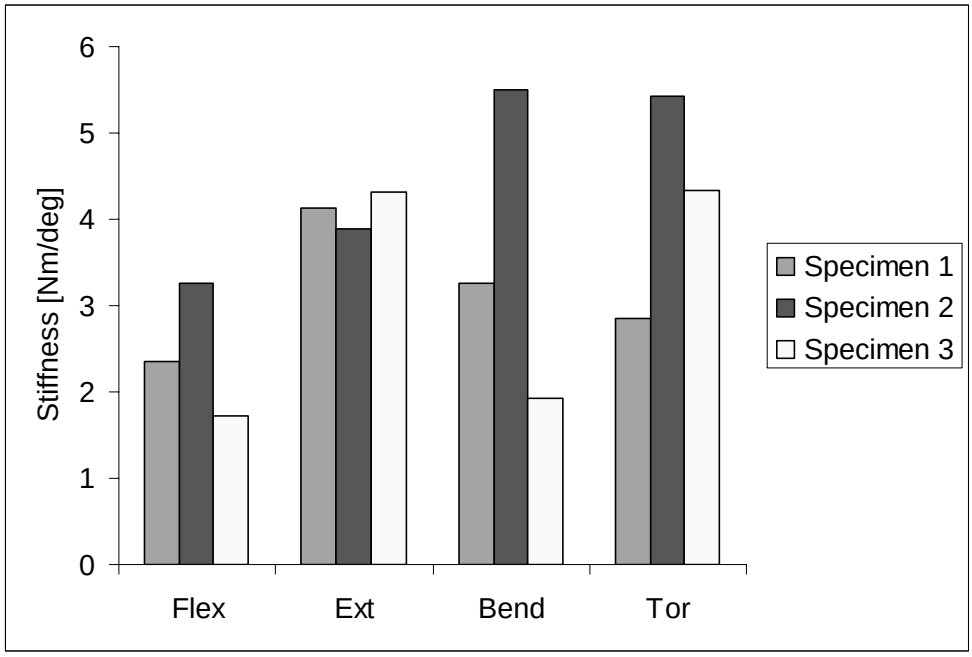

Figure B-6: Stiffness Comparison Between the Different Treated Specimens

Appendix C – Tables Related to Statistics and Experimental Data

Table C-1: Range of Motion Test Results for Individual Specimens During Extension Loading

	Intact [Nm]	Treatment [Nm]
Specimen 1	2.081623	0.983444
Specimen 2	2.800083	1.035348
Specimen 3	1.650000	1.070861
Mean	2.177235	1.029884
Standard Deviation	0.580972	0.043964

Table C-2: Range of Motion Test Results for Individual Specimens During Flexion Loading

	Intact [Nm]	Treatment [Nm]
Specimen 1	3.223510	1.589901
Specimen 2	5.419868	1.068129
Specimen 3	4.198759	2.117136
Mean	4.280712	1.591722
Standard Deviation	1.100470	0.524506

Appendix C. (Continued)

Table C-3: Range of Motion Test Results for Individual Specimens During Bending Loading

	Intact [Nm]	Treatment [Nm]
Specimen 1	5.479967	2.955795
Specimen 2	6.083692	1.813907
Specimen 3	6.602732	4.583941
Mean	6.055464	3.117881
Standard Deviation	0.561915	1.392112

Table C-4: Range of Motion Test Results for Individual Specimens During Torsion Loading

	Intact [Nm]	Treatment [Nm]
Specimen 1	4.114073	2.513245
Specimen 2	1.491557	1.256623
Specimen 3	1.928642	1.688245
Mean	2.511424	1.819371
Standard Deviation	1.405035	0.638491

Appendix C. (Continued)

Table C-5: Stiffness Test Results for Individual Specimens During Extension Loading

	Intact [Nm]	Treatment [Nm]
Specimen 1	2.155369	4.125380
Specimen 2	1.207111	3.882020
Specimen 3	2.661620	4.321470
Mean	2.008033	4.109623
Standard Deviation	0.738363	0.220149

Table C-6: Stiffness Test Results for Individual Specimens During Flexion Loading

	Intact [Nm]	Treatment [Nm]
Specimen 1	1.259533	2.343231
Specimen 2	0.755765	3.266234
Specimen 3	0.944333	1.725766
Mean	0.986544	2.445077
Standard Deviation	0.254523	0.775267

Appendix C. (Continued)

Table C-7: Stiffness Test Results for Individual Specimens During Bending Loading

	Intact [Nm]	Treatment [Nm]
Specimen 1	1.680425	3.264725
Specimen 2	1.498587	5.496485
Specimen 3	1.359610	1.931985
Mean	1.512874	3.564398
Standard Deviation	0.160884	1.801047

Table C-8: Stiffness Test Results for Individual Specimens During Torsion Loading

	Intact [Nm]	Treatment [Nm]
Specimen 1	1.832627	2.859055
Specimen 2	5.340553	5.433570
Specimen 3	3.735976	4.329021
Mean	3.636385	4.207215
Standard Deviation	1.756083	1.291572

Appendix C. (Continued)

Table C-9: Summary of the Single Factor ANOVA Performed on the Range of Motion Specimens During Extension Loading

Groups	*Count*	*Sum*	*Average*	*Variance*
Column 1	3	6.531705	2.177235	0.337529
Column 2	3	3.089652	1.029884	0.001933

ANOVA

Source of Variation	*SS*	*df*	*MS*	*F*	*P-value*	*F crit*
Between Groups	1.974622	1	1.974622	11.63384	0.027006	7.708647
Within Groups	0.678924	4	0.169731			
Total	2.653545	5				

Appendix C. (Continued)

Table C-10: Summary of the Single Factor ANOVA Performed on the Range of Motion Specimens During Flexion Loading

Groups	*Count*	*Sum*	*Average*	*Variance*
Column 1	3	12.84214	4.280712	1.211034
Column 2	3	4.775166	1.591722	0.275106

ANOVA

Source of Variation	*SS*	*df*	*MS*	*F*	*P-value*	*F crit*
Between Groups	10.846	1	10.846	14.5962	0.01877	7.708647
Within Groups	2.972281	4	0.74307			
Total	13.81828	5				

Appendix C. (Continued)

Table C-11: Summary of the Single Factor ANOVA Performed on the Range of Motion Specimens During Lateral Bending Loading

Groups	*Count*	*Sum*	*Average*	*Variance*
Column 1	3	18.16639	6.055464	0.315748
Column 2	3	9.353643	3.117881	1.937975

ANOVA

Source of Variation	*SS*	*df*	*MS*	*F*	*P-value*	*F crit*
Between Groups	12.94409	1	12.94409	11.48685	0.02755	7.708647
Within Groups	4.507446	4	1.126861			
Total	17.45154	5				

Appendix C. (Continued)

Table C-12: Summary of the Single Factor ANOVA Performed on the Range of Motion Specimens During Axial Rotation Loading

Groups	*Count*	*Sum*	*Average*	*Variance*
Column 1	3	7.534272	2.511424	1.974124
Column 2	3	5.458113	1.819371	0.407671

ANOVA

Source of Variation	*SS*	*df*	*MS*	*F*	*P-value*	*F crit*
Between Groups	0.718406	1	0.718406	0.603248	0.480711	7.708647
Within Groups	4.763589	4	1.190897			
Total	5.481995	5				

Appendix C. (Continued)

Table C-13: Summary of the Single Factor ANOVA Performed on the Stiffness Specimens During Extension Loading

Groups	*Count*	*Sum*	*Average*	*Variance*
Column 1	3	6.0241	2.008033	0.54518
Column 2	3	12.32887	4.109623	0.048465

ANOVA

Source of Variation	*SS*	*df*	*MS*	*F*	*P-value*	*F crit*
Between Groups	6.62502	1	6.62502	22.31977	0.009142	7.708647
Within Groups	1.187291	4	0.296823			
Total	7.812311	5				

Appendix C. (Continued)

Table C-14: Summary of the Single Factor ANOVA Performed on the Stiffness Specimens During Flexion Loading

Groups	*Count*	*Sum*	*Average*	*Variance*
Column 1	3	2.959631	0.986544	0.064782
Column 2	3	7.335231	2.445077	0.60104

ANOVA

Source of Variation	*SS*	*df*	*MS*	*F*	*P-value*	*F crit*
Between Groups	3.19098	1	3.19098	9.585091	0.036363	7.708647
Within Groups	1.331643	4	0.332911			
Total	4.522623	5				

Appendix C. (Continued)

Table C-15: Summary of the Single Factor ANOVA Performed on the Stiffness Specimens During Lateral Bending Loading

Groups	*Count*	*Sum*	*Average*	*Variance*
Column 1	3	4.538622	1.512874	0.025884
Column 2	3	10.69319	3.564398	3.243769

ANOVA

Source of Variation	*SS*	*df*	*MS*	*F*	*P-value*	*F crit*
Between Groups	6.313127	1	6.313127	3.86165	0.120845	7.708647
Within Groups	6.539305	4	1.634826			
Total	12.85243	5				

Appendix C. (Continued)

Table C-16: Summary of the Single Factor ANOVA Performed on the Stiffness Specimens During Axial Rotation Loading

Groups	*Count*	*Sum*	*Average*	*Variance*
Column 1	3	10.90916	3.636385	3.083826
Column 2	3	12.62165	4.207215	1.668159

ANOVA

Source of Variation	*SS*	*df*	*MS*	*F*	*P-value*	*F crit*
Between Groups	0.48877	1	0.48877	0.205712	0.673666	7.708647
Within Groups	9.503972	4	2.375993			
Total	9.992742	5				

Appendix D – Publications Related to the Dissertation Research

1) In Press

   1.1) Finite Element Analysis of Dynamic Instrumentation Demonstrates Stress Reduction in Adjacent Level Discs. Published in SAS Journal

2) Manuscripts in Preparation

   2.1) Biomechanical Testing of Percutaneous Lumbar Facet Fusion Allograft—A Pilot Study. To be submitted to Journal of Biomechanics

   2.2) A comparison between in-vivo and in-vitro intradiscal pressures. To be submitted to Spine Journal

Authors Include:

Antonio E. Castellvi, Deborah H. Clabeaux, Hao Huang,

William E. Lee, Sunil Saigal, David Pienkowski

ABOUT THE AUTHOR

Tov Inge Vestgaarden completed his Bachelors degree in Mechanical Engineering, as well as dual Master degrees in Mechanical and Biomedical Engineering. During his graduate studies, the author concentrated his research in material sciences and mechanics. In his doctoral research he applied these sciences in the field of spine biomechanics. During his studies, he was also teaching undergraduate courses. He was nominated and received the Provost Commendation For Outstanding Teaching By A Graduate Teaching Assistant for his teaching accomplishments.

He has also submitted and been accepted to present his research at the World Spine Conference in 2007. As well as having publication accepted for publication in peer reviewed journal.

Prior to his education, Tov I. Vestgaarden served in the Royal Norwegian Air force, where he was honorably discharged.